United States
Environmental Protection
Agency

EPA/600/R-08/012 | January 2008 | www.epa.gov/ord

Evaluation of In-Room Air Cleaners for Building Protection

FINAL REPORT

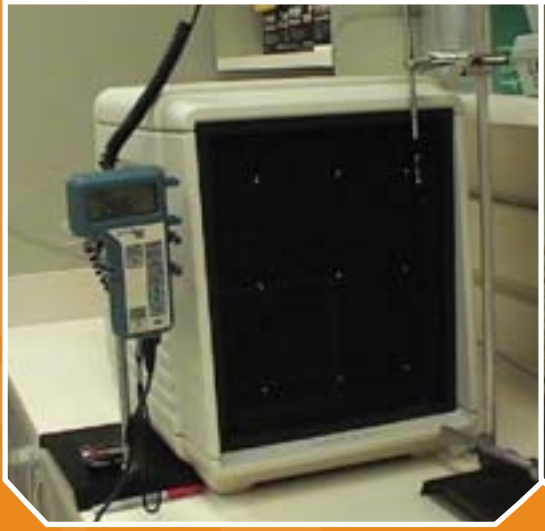

Office of Research and Development
National Homeland Security Research Center

EPA/600/R-08/012 | January 2008 | www.epa.gov/ord

FINAL REPORT ON

Evaluation of In-Room Air Cleaners for Building Protection

Contract No. GS-10F-0275K

Task Order 1105

Prepared for

Joseph Wood and Les Sparks, Project Officers

U.S. ENVIRONMENTAL PROTECTION AGENCY
Research Triangle Park, NC

January 2008

Prepared by

Vladimir Kogan (614) 424-7970
Chris Harto (614) 424-3025
David J. Hesse (614) 424-5610
Kent C. Hofacre (614) 424-5639

BATTELLE COLUMBUS OPERATIONS
505 King Avenue
Columbus, Ohio 43201-269

Office of Research and Development
National Homeland Security Research Center, Decontamination and Consequence Management Division

Disclaimer

The U.S. Environmental Protection Agency through its Office of Research and Development funded this research. It has been subject to an administrative review but does not necessarily reflect the views of the Agency. No official endorsement should be inferred. EPA does not endorse the purchase or sale of any commercial products or services.

Table of Contents

EXECUTIVE SUMMARY ..... **viii**
1.0 INTRODUCTION **1**
2.0 AIR CLEANER SELECTION **1**
3.0 EXPERIMENTAL STUDY **3**
3.1 Single-Pass Testing 3
3.1.1 Test Setup 3
3.1.2 Test Procedure 8
3.1.3 Data Analysis 9
3.1.4 Test Results and Discussion 10
3.2 In-Room Testing of Air Cleaners 16
3.2.1 Test Setup 16
3.2.2 Test Procedure 18
3.2.3 Data Analysis 19
3.2.4 Results and Discussion 19
4.0 MODELING STUDY **23**
4.1 FLUENT CFD Modeling 23
4.1.1 Results 23
4.2 Perfectly-Mixed Zone Analysis 25
5.0 CONCLUSIONS AND RECOMMENDATIONS **27**
6.0 REFERENCES **29**
APPENDIX A: AIR CLEANER SELECTION **A-1**
APPENDIX B: CFD MODELING, DETAILED METHODOLOGY, AND RESULTS **B-1**
APPENDIX C: QUALITY ASSURANCE **C-1**

List of Tables

Table 1. CADR Characteristics of Selected Air Cleaners 1
Table 2. Air Cleaner Specifications 2
Table 3. Test Matrix for Single-Pass Evaluation of Air Cleaners 3
Table 4. SMPS Size Channels 5
Table 5. Velocity Characteristics of the ESP Air Cleaner 10
Table 6. ESP Air Cleaner Flow Rates 11
Table 7. Flow Characteristics of the HEPA Filter 11
Table 8. In-Room Test Matrix 16
Table 9. Calculated Decay Constants 21
Table 10. Collected Filter Masses 22

List of Figures

Figure 1. Electrostatic Precipitator and HEPA Air Cleaner 2
Figure 2. Schematic of the Single-Pass Efficiency Test Apparatus 3
Figure 3. Airflow Measurements for ESP Air Cleaner 4
Figure 4. Aerosol Sampling Instruments, TSI SMPS and Climet CI-500 5
Figure 5. Representative Diameter Distributions of Test Aerosols Obtained Using TSI SMPS and Climet CI-500 7
Figure 6. Plots of Bias Correction Factor (*R*) and Sampling Variability (*V*) 9
Figure 7. Local Velocities of the ESP Air Cleaner 10
Figure 8. Local Velocities of the HEPA Filter 11
Figure 9. Filtration Efficiency for the ESP Air Cleaner 12
Figure 10. Filtration Efficiency for the HEPA Filter 12
Figure 11. ESP Bioaerosol Filtration Efficiency 14
Figure 12. HEPA Bioaerosol Filtration Efficiency 14
Figure 13. Downstream Particle Counts From ESP Bioaerosol Test, Run 2 15
Figure 14. Upstream Particle Counts From ESP Bioaerosol Test, Run 2 15
Figure 15. Test Chamber for In-Room Experiments 16
Figure 16. In-Room Test Configuration A 17
Figure 17. In-Room Test Configuration B 17
Figure 18. In-Room Test Configuration C 18
Figure 19. Concentration vs. Time Plots, Individual Configurations 20
Figure 20. Concentration vs. Time Plot, Averaged Data 20
Figure 21. Size-Resolved Concentration vs. Time 21
Figure 22. Collected Filter Masses 22
Figure 23. CFD Model Results 24
Figure 24. Filter Masses From CFD Calculations 24
Figure 25. Well-Mixed Zone Model Results 25

List of Acronyms

AHAM	Association of Home Appliance Manufacturers
Bg	*Bacillus globigii*
CADR	Clean Air Delivery Rate
CFD	computational fluid dynamics
CV	coefficient of variation (computed as the standard deviation divided by the mean)
ESP	electrostatic precipitator
HEPA	high-efficiency particulate air
HVAC	heating, ventilation, and air conditioning
KCl	potassium chloride
LES	large eddy simulation
PM	particulate matter
QAPP	Quality Assurance Project Plan
SMPS	scanning mobility particle sizer

Executive Summary

This report describes the experiments and modeling conducted to determine the effectiveness of commercially available in-room air cleaners (i.e., particulate matter [PM] filtration devices) in mitigating the impact of an aerosolized biological threat agent attack on a building. In one set of experiments, two air cleaners were evaluated for their single-pass filtration efficiency as a function of airflow rate, particle diameter (ranging from 0.03 μm to 10 μm), and type of particle (an inert aerosol and a bioaerosol). One of the air cleaners tested was a high-efficiency particulate air (HEPA) filtration device, and the other was an electrostatic precipitator (ESP) air cleaner. Following the single-pass experiments, the HEPA filter was further evaluated to verify its effectiveness in reducing in-room PM levels.

For the single-pass testing, the ESP air cleaner displayed a pronounced minimum in filtration efficiency for particles ~ 0.2 μm diameter, consistent with the principles of electrostatic precipitation. Also, the single-pass efficiency of the ESP air cleaner was found to decrease with increasing flow rate through the unit, most likely due to the decreasing residence time of the particles in the charging and deposition zones of the collector.

For the HEPA filter, no noticeable effect of flow rate on the filtration efficiency of the unit was observed, but an unexpected drop in efficiency was observed for particles below 0.3 μm in diameter. This observation could be explained by the probability that some leaks developed around the filter due to its relatively loose fit in the single-pass test apparatus.

Both air cleaners' filtration efficiencies for particles with diameters smaller than approximately 0.04 μm were lower than expected. No difference in the air cleaners' filtration efficiencies was observed for the biological and inert aerosols having similar particle diameters.

For the in-room experiments, the HEPA filter was evaluated in a test chamber under four configurations. In these experiments, the PM concentration decay rate was determined by continuously monitoring the aerosol concentration at a particular location in the room, using a real-time particle counter. Also, average PM levels occurring in the room were determined using filter samples taken at five different locations.

The effectiveness of an in-room air cleaner under typical operating settings depends on three principal characteristics: 1) the single-pass filtration efficiency, 2) the airflow rate through the filter, and 3) the airflow pattern that the cleaner induces in the room. While the first two characteristics can be determined from some straightforward measurements, such as those used in this study, the airflow pattern in the room is also dependent upon other factors, such as room size and shape; heating, ventilation, and air conditioning (HVAC) characteristics; furnishings; leak patterns; and the presence of mixing fans. In this research, some of these factors were investigated using the HEPA filter.

The HEPA filter tested was found to provide significant protection with respect to the contaminant concentration profile in the test room, when compared to the case when the air cleaner was not operating. This observation was expected and illustrates the usefulness of in-room air cleaners to reduce ambient PM levels following an attack with an aerosolized threat agent. The location of the air cleaner relative to the aerosol source was found to have a minimal impact. The addition of an office desk and a chair in the test chamber also did not appear to noticeably alter the performance of the air cleaner. Overall, the HEPA filter provided reasonable mixing conditions in the test room, although some variability in the PM levels measured at different locations within the chamber was observed.

Following the completion of the experimental phase of the project, model calculations were performed using computational fluid dynamics (CFD) for one of the specific in-room test configurations investigated in this work. In addition, non-CFD calculations were performed for the test conditions, using the perfectly-mixed zone modeling approach.

CFD model simulations can offer a viable alternative to field tests because of the demonstrated ability of this technique to predict the general trends of contaminant behavior in various indoor settings. The CFD model did a reasonable job of modeling the variability of the concentration of PM within the chamber, although it overestimated the concentration decay rate at the specified location. The main issue associated with this application of CFD is the broad spectrum of flow regimes evolving within the room, ranging from laminar to fully turbulent conditions. This requires specification of different turbulence closure models, such as large eddy simulations (LES) for describing large flow recirculation patterns. The model also requires more refined schemes to adequately describe the dispersion of PM in the aerosol generation and air cleaner exhaust zones.

1.0 Introduction

This report describes experimental and modeling efforts to determine the effectiveness of commercially available in-room air cleaners in mitigating the impact of an aerosolized biological agent attack on a building. The project consisted of four principal phases. In the first phase, two representative air cleaners were selected for experimental evaluation, one based on the high- efficiency particulate air (HEPA) filtration mechanism and one using electrostatic precipitation (ESP). In the second phase of the project, the selected air cleaners were evaluated for their single-pass filtration efficiency for both an inert aerosol and a bioaerosol. In the third phase, one of the air cleaners was selected for evaluation of its effectiveness in reducing PM levels in a test chamber designed to simulate "in-room" conditions. Finally, in the fourth phase, both a computational fluid dynamics (CFD) model and calculations based on a "well-mixed volume" model were used for theoretically evaluating the effectiveness of in-room air cleaners. This experimental portion of this project was performed according to a test/quality assurance project plan (QAPP; see Appendix C).

2.0 Air Cleaner Selection

The first step in the overall project was to select the air cleaners for testing. A list of candidate air cleaners was obtained by performing a brief market survey through the Internet. Based on the Internet search, the manufacturers of the candidate air cleaners were contacted to collect the detailed performance and specification data on their products. Two air cleaners were then selected, based on the following selection criteria:

- Operating principle: one HEPA filter type air cleaner and one ESP type air cleaner
- Off-the-shelf commercial availability of a high-quality brand
- High aerosol collection efficiency, as specified by the manufacturer, preferably higher than 99% efficiency for 0.3 μm aerosol particles
- Airflow rate capacity on the order of 300 ft^3/min (0.142 m^3/s), or 7 to 10 air exchanges per hour for a single-room of 8 ft x 16 ft x 8 ft (2.4 m x 4.9 m x 2.4 m) — the size of the test facility available at Battelle
- Having at least three-stage adjustable airflow capability

Most room air cleaners on the market are certified under the Room Air Cleaner Certification Program, which is sponsored by the Association of Home Appliance Manufacturers (AHAM). Under this program, room air cleaners are characterized using the Clean Air Delivery Rate (CADR), which determines how effectively they remove different particulate pollutants such as tobacco smoke, dust, and pollen. One hundred seventy-four different models of room air cleaners from 18 manufacturers are currently certified under the program. Among them, only one was an ESP-type air cleaner, so it was selected for testing under this program. Another air cleaner, the HEPA filter-type air cleaner, was selected for testing because it had a similar CADR rating to the ESP. The CADR values for the two air cleaners are shown in Table 1; additional specification parameters are listed in Table 2. It should be noted that these two air cleaners are also the top two room air cleaners recommended by *Consumer Reports*. Pictures of the two selected air cleaners are shown in Figure 1.

Table 1. CADR Characteristics of Selected Air Cleaners

Type	CADR cfm (m^3/s)		
	Tobacco Smoke (0.09 to 1.0 μm)	Dust (0.5 to 3 μm)	Pollen (5 to 11 μm)
ESP	300 (.142)	325 (.153)	370 (.175)
HEPA	320 (.151)	330 (.156)	330 (.156)

Table 2. Air Cleaners Specifications

Type	ESP	HEPA
Fan Flow Rate	Low 225 cfm (0.106 m^3/s) Medium 275 cfm (0.130 m^3/s) High 365 cfm (0.172 m^3/s) (flows specified by manufacturers)	Low 275 cfm (0.130 m^3/s) Medium 340 cfm (0.160 m^3/s) High 440 cfm (0.208 m^3/s) (flows measured)
Dimensions	0.48 m H x 0.38 m L x 0.55 m W	0.56 m H x 0.46 m L x 0.28 m W
Initial Cost	$490	$260
Operating Costs (energy use)	$62/yr (based on 90W power consumption, assuming 24-hr operation on high flow at a cost of 7.77 ¢/kwhr)	Energy consumption not specified
Maintenance Costs	None specified	$80/yr for replacement filter

Figure 1. Electrostatic Precipitator (left) and HEPA Filter (right)

The selected air cleaners were tested as received, without conditioning. It is realized that performance of air cleaners containing an ESP element will degrade with accumulation of certain aerosols, such as oil aerosols, silicon oxide particles, etc. However, investigating the effect of potential degradation of the performance of air cleaners due to aerosol loading was beyond the scope of this study. More detail on the selection of the air cleaners, the AHAM standard, and the definition of CADR is provided in Appendix A.

3.0
Experimental Study

3.1 Single-Pass Testing

The purpose of the single-pass testing was to characterize the filtration efficiencies of the two selected air cleaners for a single pass of aerosol through the unit. The goal was to characterize the efficiency of the units over a range of flow rates and across an aerosol diameter range from 0.03 to 10 μm. This was achieved by placing the unit within a sealed flow duct and measuring the size-resolved aerosol concentration upstream and downstream of the unit with a particle counter. The units were characterized for both an inert potassium chloride (KCl) aerosol and a bioaerosol consisting of *Bacillus globigii* (Bg) spores.

Table 3. Test Matrix for Single-Pass Evaluation of Air Cleaners

Type of Aerosol	Size (Diameter) Range (μm)	Air Capacity	HEPA (# of tests)	ESP (# of tests)
Inert Aerosol (KCl particles)	0.03 to 0.5	high	2	2
		medium	2	2
		low	2	2
	0.3 to 10	high	2	2
		medium	2	2
		low	2	2
Bioaerosol (Bg spores)	~ 1	medium	3	3

3.1.1 Test Setup

3.1.1.1 Inert Aerosol In order to adequately characterize the air cleaners over the full range of particle diameters, the inert aerosol testing was completed in two stages. During the first stage, the filtration efficiency was measured for particles ranging from 0.03 to 0.5 μm. During the second stage, the filtration efficiency was characterized for particles ranging from 0.3 to 10 μm . For each size range, the single-pass efficiency was determined at three rates of airflow through the air cleaners (low, medium, and high – see Table 2). Duplicate tests were conducted for each experimental condition. The complete test matrix, including bioaerosol tests performed in triplicate, is shown in Table 3.

A test system, conforming to the dimensions of the air cleaners, was constructed out of Plexiglas to test the single-pass efficiency of the air cleaners. A schematic of the test system is illustrated in Figure 2. This system was designed for testing in-room air cleaners that contain their own air-handling means, which requires that air pressure be close to ambient in the vicinity of both the inlet and outlet locations of the units so that the air cleaner design flow rates are not affected by the test system. It was also designed to facilitate testing air cleaners using not only inert aerosols but also biological aerosols. Custom duct sections were fabricated for each air cleaner to ensure a tight fit with the flow section of the test system.

Figure 2. Schematic of the Single-Pass Efficiency Test Apparatus

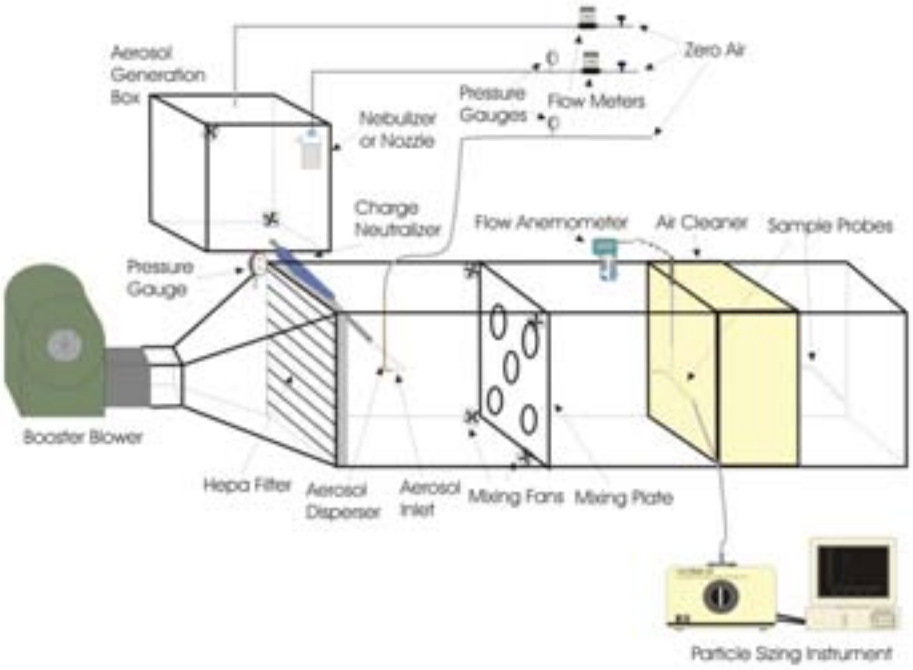

Before performing the single-pass filtration efficiency testing, airflow rates were estimated for each of the three settings for both test air cleaners. This was done using a hot-wire anemometer to measure air velocity at nine points that were identified in the middle of nine equal, representative areas across the airflow grilles. This was done for both the inlet and outlet locations of both air cleaners. The mean flow velocity was calculated using the nine velocity values obtained for both the inlet and outlet flows. The flow rate was then calculated by multiplying the mean velocity by the flow area. Figure 3 shows the setup used for determining the flow rate.

Figure 3. Airflow Measurements for ESP Air Cleaner

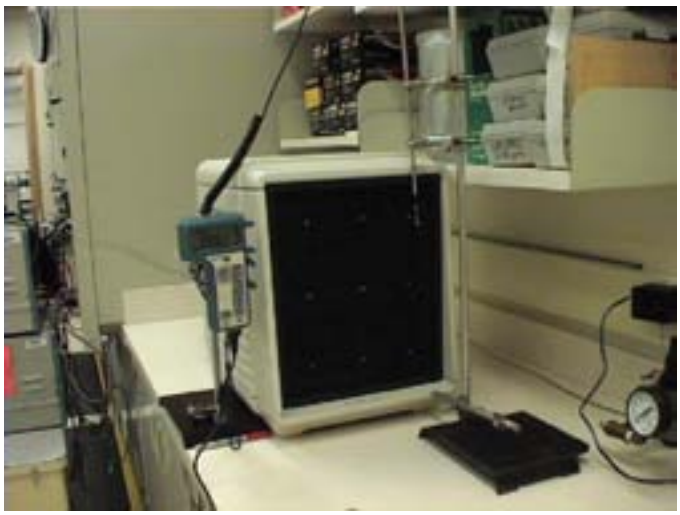

To ensure that the test rig components did not alter the natural airflow of the room air cleaner, a boosting blower was installed upstream of the test section. During a test, the output of the boosting blower was adjusted so that the air velocity measured for the test air cleaner was maintained close to that obtained during the air cleaner flow characterization phase (± 10%). For the ESP, the velocity was matched upstream in the middle of the unit. For the HEPA filter, however, the air velocity was found to be too variable across the inlet to be accurately represented by a single location. Therefore, its mean flow velocity was determined by taking the average of measurements at each of the nine outlet locations used for the airflow characterization. The blower was adjusted until this average was ± 10% of the average obtained for the free-standing unit.

The challenge aerosol was generated using a Baxter Co. Airlife™ nebulizer. A 5% KCl solution was used to generate the smaller aerosol, and a 20% solution was used to generate the larger aerosol. Dry, clean air was supplied to the nebulizer. The airflow to the nebulizer was controlled with a needle valve, and its pressure and flow rate were monitored. The nebulizer was connected to a large drying chamber to allow the droplets to dry before they reached the test duct. An additional flow of dry air was supplied to the chamber to assist in drying the particles and to carry them into the test duct. Before entering the test duct, the particles were passed through an aerosol neutralizer (containing Kr-85, 10 mCi) to reduce their charge level. This was necessary as aerosol particles have a tendency to collect static charge, which may influence their filtration characteristics.

One of the requirements of this testing was to establish not only undisturbed, natural airflows through the air cleaners, but also to provide uniform aerosol concentration across their inlets. In order to achieve efficient mixing of particles across the test duct, the aerosol was injected into the duct against the airflow, as illustrated in Figure 2. In addition, four small mixing fans and a turbulence enhancement plate were installed upstream of the air cleaners to improve mixing efficiency. However, due to the high air velocity in the duct, combined with the short duct length, an additional dispersion means was required. An auxiliary aerosol disperser was fabricated using quarter-inch diameter copper tubing, which was placed coaxial to the aerosol delivery tube in the proximity of its injection point. The tube was plugged, and a number of small holes were drilled radially near the end of the tube. Pressurized air was passed through the tube and out through the holes at high velocity. The resulting flow was designed to entrain the aerosol as it entered the duct and carry it away from the center. This setup allowed for a uniform challenge concentration to be achieved at the air cleaner test location.

Before the tests were conducted, the uniformity of aerosol concentration was confirmed. To achieve this, aerosol measurements were performed upstream of the air cleaner, at a cross-sectional plane perpendicular to the flow. The cross-section was divided into nine equal representative areas, and concentration was measured at the center of each area. The mean concentration and the coefficient of variation (CV, computed as the standard deviation divided by the mean) of the nine corresponding grid point concentration values was then calculated. The maximum acceptable CV value was set at 15%. If the measured CV exceeded 15%, the mixing measures were adjusted, and the uniformity was recharacterized until the requirement of CV less than 15% was met. This uniformity test was performed for one flow rate for both aerosol diameter ranges.

These tests were performed before the air cleaner was installed in the duct, with the airflow generated by the booster blower only in order to test the effectiveness of mixing in the duct independent of the individual air cleaners. The apparatus was designed to minimize its effect on the performance of the air cleaner, and mixing was designed to take place in a separate section upstream of the air cleaner location. Introduction of the air cleaner into the duct was assumed to have no negative impact on the uniformity in the challenge concentration. The justification for this assumption was that if the concentration was uniform upstream of the air cleaner location then it was thought to be unlikely that the air cleaner would measurably affect the concentration profile based on basic mass transport principles.

During a test, the upstream and downstream concentrations were measured at two fixed locations along the duct centerline. This was considered adequate for the purposes of this study because that concentration CV in the cross-sections was required to be less than 15%. The spatial variability

in flow velocities introduced by the air cleaners was assumed to have a minimal effect on the results of this study because a uniform concentration remains uniform across noncompressible flow regardless of velocity. The aerosol was sampled from two identical sample probes. These probes were fabricated from quarter-inch stainless steel tubing bent 90 degrees and tapered at the inlet and were inserted into the test duct with the inlet facing the flow. The particle counter was then attached to the appropriate sample probe when a measurement was to be taken. The aerosol concentration was measured by using two different instruments, one for each aerosol diameter range.

The small aerosol was sampled using a TSI scanning mobility particle sizer (SMPS). This instrument consists of an electrostatic classifier, which is used to separate particles by size, and a condensation particle counter, which counts the particles. The detection range of the instrument is 20 to 10^7 particles/cm^3. In the test configuration, this instrument had a sample rate of 0.3 L/min and a sample time of two minutes. The design of the instrument is such that the particles are counted one size channel at a time, thus each size channel is sampled for only a fraction of the two-minute sampling time. The effective range of particle diameters measured by the instrument was 0.02 to 0.56 microns (only values from 0.0237 to 0.316 microns were used due to low particle concentrations of test aerosol). Table 4 shows the breakdown of the instrument size channels and their upper and lower limits. All values are in nanometers. The SMPS was controlled by a computer, and all data were collected using the TSI's "Aerosol Instrument Manager" software. The data collected were then transferred to Excel using the "cut and paste" function for further analysis.

The large aerosol was sampled using a Climet CI-500 laser particle counter. This unit is designed to detect light scattered by aerosol particles as they pass through the measuring volume defined by the width of the instrument's laser beam. In order to ensure that only one particle passes through the measuring volume at a time, the CI-500 has an upper detection limit of up to 10^7 particles/ft^3 (~350 particles/cm^3). This, however, did not introduce an aerosol counting problem because the instrument samples the aerosol at a relatively high airflow rate of 2.83 L/min, and its sampling time was set to one minute. The size range of the instrument is 0.3 to 10 microns, which is broken down into five size channels. Unlike the SMPS, the CI-500 measures all particle sizes simultaneously. During the single-pass tests, the unit was operated from the control panel on the front of the instrument. The data collected were stored in the unit's internal memory during the test, after which they were downloaded into Excel, using the software provided with the instrument.

Figure 4 shows photographs of the two particle counters used in this work. Figure 5 shows typical distributions of the fine and "coarse" test aerosols obtained with the SMPS and CI-500 particle counters, respectively. The two selected instruments measure particles based upon different physical properties: electrical mobility in the case of the SMPS and light scattering in the case of the Climet. This can lead to a small difference in the particle size measured for a specific particle measured by both instruments; however, this error is reduced because particles sizes are binned over a range of particle sizes. Also, this will not affect the efficiency measurements, which compare concentration in the same size bin.

Table 4. SMPS Size Channels (all values in nanometers)

Size Channel	20.5	27.4	36.5	48.7	64.9	86.6	115	154	205	274	365	487
Lower Limit	17.8	23.7	31.6	42.2	56.2	75.0	100	133	178	237	316	422
Upper Limit	23.7	31.6	42.2	56.2	75	100	133	178	237	316	422	562

Figure 4. Aerosol Sampling Instruments, TSI SMPS (left) and Climet CI-500 (right)

3.1.1.2 Bioaerosol The single-pass filtration efficiency of the two test air cleaners was also evaluated using a biological aerosol. The same test apparatus described above was used with the bioaerosol challenge. A suspension of Bg spores, which are elongated particles with approximate dimensions of (0.7–0.8) μm x (1.0–1.5) μm, were used to generate airborne microorganisms in the bioaerosol tests. The tests were performed for each air cleaner at the medium flow rate. The purpose of this testing was to determine whether there was a noticeable difference in the effectiveness of the air cleaners in handling biological particles versus equally sized inert particles.

The Bg spores were selected for this testing because they are a well-accepted surrogate for anthrax spores, having similar dimensions and viability characteristics. They can remain viable under a variety of harsh environmental conditions. The Bg spores have a mass median aerodynamic diameter of approximately 1 μm and therefore have a relatively high probability of penetration through furnace filters. The Bg slurry was prepared by adding a dry powder of Bg spores to high-purity water. The target concentration of spores in the slurry was approximately 10^7 CFUs (colony forming units)/mL in order to achieve a sufficiently high challenge concentration of Bg in the air. At the same time, this concentration of microorganisms in liquid suspension also provided favorable conditions for single-spore aerosolization. Considering, for example, that the nebulizer generates liquid droplets with diameters on the order of 10 μm, aerosolization of a suspension of 10^7 CFU/mL results in an aerosol containing approximately 0.01 spores/drop, suggesting a very low probability of producing multiple-spore particles. The actual concentration of spores in the test slurry was determined by plating an aliquot of the slurry and counting the resulting colonies, which resulted in a concentration of 4.4 x 10^7 CFU/mL. The Bg spores were aerosolized using a Baxter Airlife™ nebulizer.

The overall aerosol concentration was measured upstream and downstream of the air cleaner using the Climet CI-500 particle counter, while concentration of Bg spores in the air was determined using water-soluble gelatin filters (Sartorius, Edgewood, NY). These filters were placed in standard 47-mm filter housings, which had been autoclaved prior to testing, and connected to the sampling probes. A vacuum pump was used to sample through the filters at a rate of 10 L/min. The Sartorius gelatin filters function in the same manner as standard membrane filters, but since they are soluble, the collected microorganisms can be plated and counted for determining their concentration in the air.

Each bioaerosol test consisted of simultaneously sampling upstream and downstream of the air cleaner with a single filter at each location. Upon completion of the test, the gelatin filters were dissolved in 10 mL of high-purity water and then diluted to an appropriate concentration before being plated on tryptone soy agar (TSA). Three plates were made from each filter, and the organisms were allowed to incubate at 36 °C for 24 hours. After the incubation period, the organisms were counted using the Qcount™ automatic plate counter (Spiral Biotech, Inc.), and the organism counts were used to calculate the filtration efficiency of the test air cleaner.

Figure 5. Representative Diameter Distributions of Test Aerosols Obtained Using TSI SMPS (a) and Climet CI-500 (b)

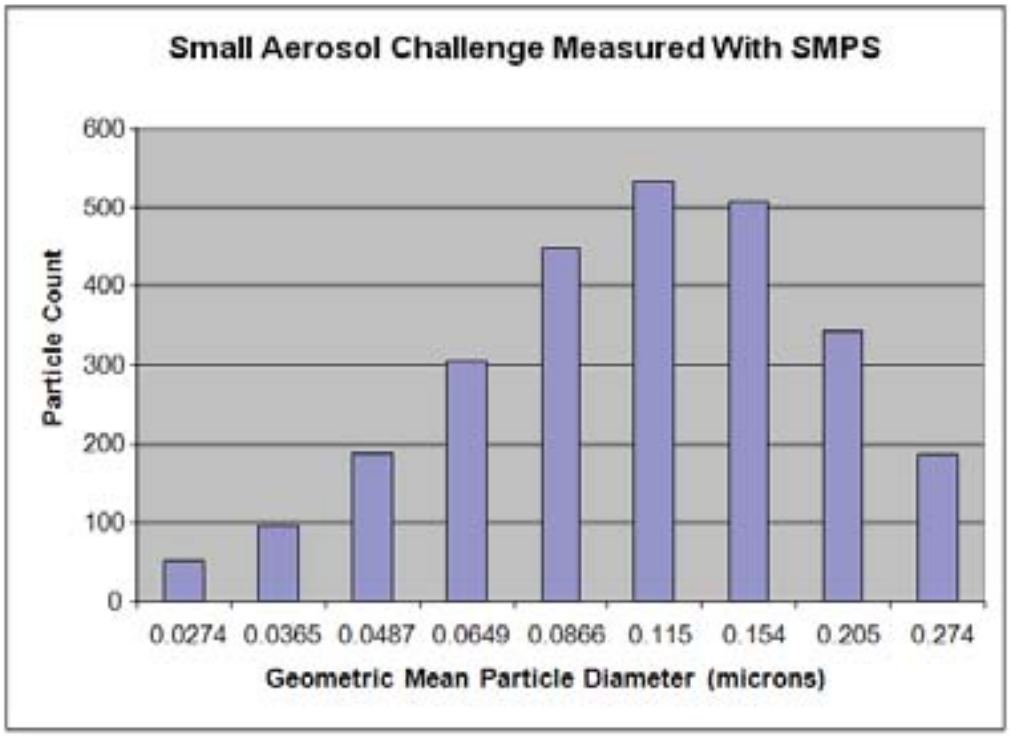

(a)

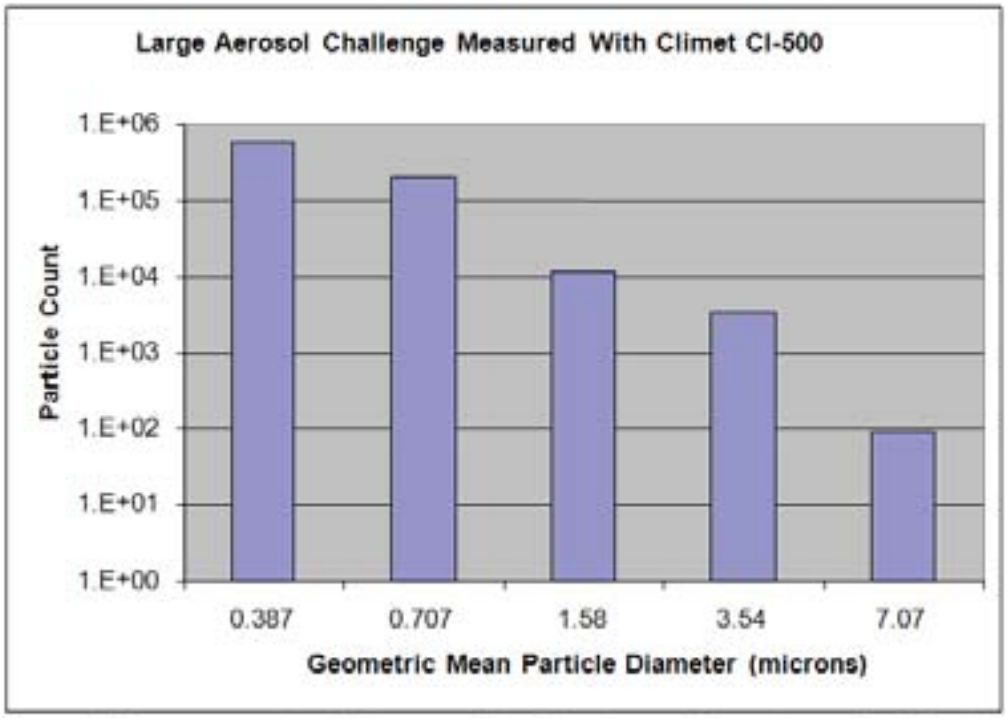

(b)

3.1.2 Test Procedure

3.1.2.1 Inert Aerosol The procedure developed for the single-pass inert aerosol testing can be broken down into two distinct stages: system startup and data collection. The startup stage consisted of turning on the equipment, establishing the correct flow within the test duct, and achieving a stable challenge aerosol concentration. The data collection stage consisted of taking three alternating measurements at both the upstream and downstream locations. This was done in order to minimize the potential effect of any temporal variability in the challenge concentration on the measurement results, as well as to obtain better statistics in the particle counts. The total particle counts from the three measurements were summed, and the ratio of total downstream to total upstream particle counts was used to calculate the fractional filtration efficiency.

The detailed test procedure was as follows:

- Turn on the aerosol counting instrument.
- Open the air supply to the aerosol disperser and turn on the mixing fans in the test duct and in the aerosol generation box.
- Turn on both the booster blower and the air cleaner and set the air cleaner to the appropriate setting.
- Set the air cleaner flow rate. Measure the air velocity using a hot-wire anemometer. If the velocity is within 10% of the velocity measured for the same unit in the free-standing configuration, record the value on the data sheet and continue. If the velocity is not within the specified range, adjust the blower setting and measure again. Repeat this process until the correct flow is achieved.
- Record the test duct pressure and the ambient temperature and humidity on the data sheet.
- Attach a cartridge HEPA filter to the inlet of the aerosol sampling instrument to make a zero count measurement and check for leaks. If the total number of particles detected is above 10, check for leaks, tighten fittings, and measure again.
- Detach the HEPA filter and attach the instrument's sampling tube to the upstream sample probe. Take an upstream background measurement. If the background is higher than 1% of the target challenge concentration, let the system run for a period of time and take the background measurements again. Then switch to the downstream sample probe and take a downstream background measurement. Use the final background measurement taken before the test in data analysis.
- Fill the Airlife™ nebulizer with the appropriate pre-prepared KCl solution and attach it to the aerosol generation box. Record the solution concentration on the data sheet.
- Turn on the nebulizer and dilution air to the mixing chamber. Record the flow rate of both the air to the nebulizer and the air to the mixing chamber, as well as the nebulizer supply pressure.
- Allow the nebulizer to run for at least 10 minutes to allow the aerosol concentration to approach steady-state.
- Attach the instrument's sample tube to the upstream sample probe and take the first measurement.
- If the large aerosol is being tested, attach the HEPA cartridge filter to the instrument and take a measurement to clear the sample line. This should be done after each upstream measurement using the Climet CI-500 because this instrument does not sample continuously. This is not necessary when using the SMPS because it does sample continuously. However, a wait time of 15 seconds should be allowed between attaching the sample tube to the sample probe and starting the measurement to allow the sample tube to clear.
- Move the sample tube to the downstream sample probe and take another measurement.
- Repeat the previous three steps two more times for a total of three measurements at each location.
- Turn off the aerosol generation system and allow the blower and air cleaner to run for a period of time before starting another test.

This procedure was followed for all inert aerosol tests for both the large and small aerosol size ranges. Test information was recorded on the test-specific data sheets kept in a three-ring binder. Data from the SMPS and Climet particle counters were transferred to Microsoft Excel™ datasheets where all subsequent data analyses were performed.

3.1.2.2 Bioaerosol The procedure for the bioaerosol tests was similar to that used in the inert aerosol testing, with the exception of the sampling process. The bioaerosol tests were performed in three sequential runs, each involving simultaneously taking an upstream and downstream filter sample. The filter samples were collected by attaching the inlet of the filter housing to the appropriate sampling probe and the outlet to a vacuum pump. The pump was then turned on and run at a flow rate of 10 L/min for a period of time estimated for each air cleaner. The sampling time was calculated based upon the measured single-pass efficiency of the air cleaner obtained using the inert aerosol and the expected challenge concentration of Bg spores in the air. These sampling times were 20 minutes for the HEPA filter and 2 minutes for the ESP. Real-time aerosol measurements were also performed using the CI-500 before each set of filter samples was taken. The real-time measurements were taken to ensure the system was operating correctly, as well as to collect additional data points.

Mean upstream and downstream concentrations of the microorganism were calculated from these replicate filter samples. Particle penetration was determined in the same manner as for the inert aerosol, by taking the ratio of the

downstream to upstream CFU concentrations in the air. Background CFU counts, obtained while running the air cleaners without bioaerosol generation, were accounted for. To eliminate possible system bias, the measured air cleaner efficiency was corrected by subtracting the background counts from the test data.

3.1.3 Data Analysis

3.1.3.1 Inert Aerosol The computation of inert-aerosol filtration efficiency was based on the ratio of the downstream to upstream particle concentrations, corrected on a channel-by-channel basis for background counts (i.e., upstream and downstream counts observed when the aerosol generator was turned off) and accounting for potential system bias by using a correction factor measured at the start of a test sequence. A minimum of one background measurement was taken at the upstream and downstream locations, and three alternating upstream and downstream measurements were taken during each test. These measurements were used for determining the air cleaner filtration efficiency by computing the observed penetration fraction ($P_{observed}$) for a given particle size:

$$P_{observed} = \frac{(D - D_b)}{(U - U_b)} \quad (1)$$

where:

D = Downstream particle concentration,

D_b = Downstream background concentration,

U = Upstream particle concentration, and

U_b = Upstream background concentration.

The background concentration measurements were not used in filtration efficiency determinations if the total number of downstream background particles counted was lower than the number of the instrument's size bins. This condition was used in order to eliminate the effect of random noise counts that may appear arbitrarily in some size bins of the instruments.

As mentioned above, to remove any potential system-level sampling bias between the upstream and downstream sampling locations, the observed penetration was adjusted by the correction factor (R):

$$P_{corrected} = P_{observed} \ / \ R \quad (2)$$

The correction factor was determined from measuring particle concentrations at the two sampling locations of the test apparatus but without the air cleaner present. Two measurements were taken at each location for each flow condition. From these measurements, the bias correction factor R, defined as the ratio of downstream particle counts to the upstream counts, was calculated for each size bin, and a linear trend line was fitted to these data.

In order to ensure that the calculated R value represented actual system bias, it was examined with respect to the variability of test data obtained during separate measurements of the upstream concentrations. This was done using upstream variability ratios, V_{xy}, which were calculated by dividing the upstream counts, x, obtained during one measurement by the upstream counts, y, obtained during another measurement under the same test conditions. There were a total of six upstream samples taken for each air cleaner at each flow rate during their filtration efficiency measurements; Run 1 consisted of samples 1, 2, and 3, and Run 2 consisted of samples 4, 5, and 6. A total of six V_{xy} values were then calculated for each size bin: V_{21}, V_{32}, V_{13}, V_{54}, V_{65}, and V_{46}. A scatter plot of all the variability ratios V_{xy} was created along with the bias correction factor R, an example of which is shown in Figure 6.

Figure 6. Plots of Bias Correction Factor (*R*) and Sampling Variability (*V*)

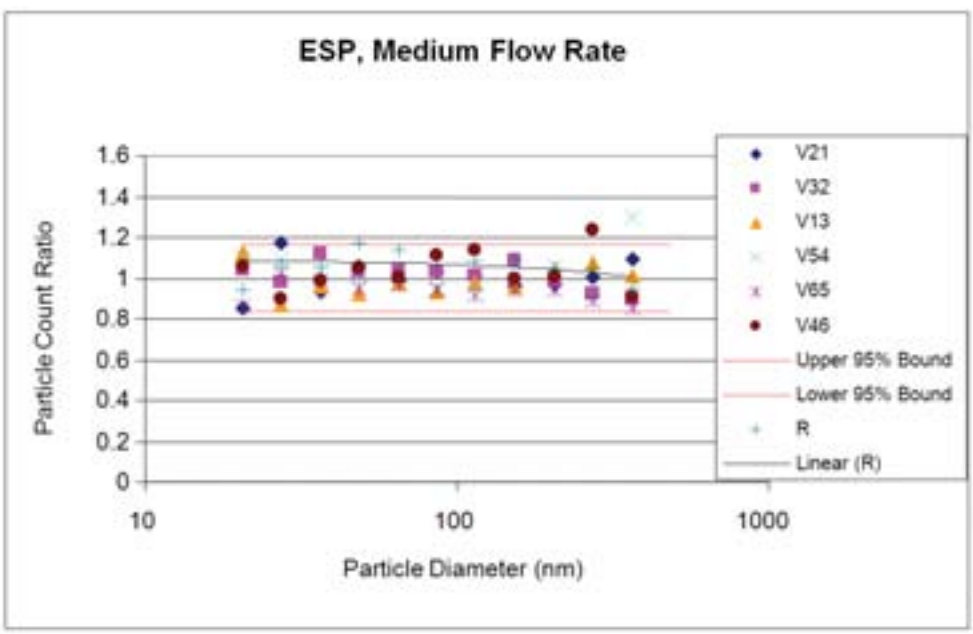

A standard deviation was then determined for the sets of sampling variability data (V_{xy}), and the upper and lower 95% confidence intervals were calculated and plotted on the graph. If the trend line of R versus particle diameter (shown in Figure 6 plotted on a logarithmic axis) was found to lie within the confidence bounds of the V_{xy} data, no correction was made to the original efficiency measurements because the measurements bias, if any, would be obscured by the variability of challenge concentration. If this was not the case, the filtration efficiency measurements were corrected by using the measured value of R in Equation 2. This procedure was followed for each combination of air cleaner, flow rate, and aerosol size range. In all cases, however, the trend line was fully within the confidence bounds, so no corrections were made to the data.

The filtration efficiency is then computed as the following:

$$\textit{Filtration Efficiency}\ (\%) = 100\ (1 - P_{corrected}) \qquad (3)$$

3.1.3.2 Bioaerosol Consistent with the inert aerosol testing, calculation of the penetration of viable microorganisms through the test air cleaner was based on the ratio of the downstream to upstream concentrations of Bg spores determined from the culturable counts on the plates. The equations used for calculating the penetration and filtration efficiency of the air cleaner are the same as described above for inert aerosol. Since no sampling bias was observed in the tests using the inert particles, no correction was applied in the determinations of bioaerosol penetration of the air cleaner.

3.1.4 Test Results and Discussion

3.1.4.1 Flow Rate Measurements The flow rates of the two test air cleaners were measured in their free-standing configurations before they were tested for their filtration performance characteristics. The flow rates were determined by using a hot-wire anemometer to measure the air velocity and calculating the flow rate based upon the flow area. The results of the air velocity measurements for the ESP air cleaner are shown graphically in Figure 7. Each square represents one of the nine imaginary flow areas chosen for this analysis. The velocity measured at the inlet is shown at the top of each square, and the velocity at the outlet is shown at the bottom. These results indicate that, by design, the flow is nonuniform across both the inlet and outlet of the air cleaner. Table 5 summarizes the test results for the average velocity upstream and downstream of the air cleaner as well as the overall average velocity for each of its three flow settings. The airflow rates were then calculated using the overall average air velocity and the flow area, which was the same for both the inlet and outlet. These values are shown in Table 6. The measured flows were considered acceptable, relative to the manufacturer's specification, for proceeding with testing.

Figure 7. Local Velocities of the ESP Air Cleaner (top inlet, **bottom outlet**)

Local Velocity (m/s)										
High				Medium				Low		
1.38	1.32	1.52		1.07	1.04	1.17		0.88	0.86	0.97
2.17	**1.83**	**2.00**		**1.74**	**1.41**	**1.62**		**1.43**	**1.13**	**1.33**
1.43	1.43	1.83		1.17	1.18	1.49		0.92	0.84	1.15
1.55	**0.21**	**1.67**		**1.25**	**0.22**	**1.15**		**0.97**	**0.16**	**0.90**
1.48	1.47	1.84		1.20	1.16	1.41		0.94	0.93	1.14
2.00	**1.70**	**2.13**		**1.85**	**1.25**	**2.02**		**1.21**	**0.92**	**1.56**

Table 5. Velocity Characteristics of the ESP Air Cleaner

Flow Setting	Average Upstream Velocity (m/s)	Average Downstream Velocity (m/s)	Overall Average Velocity (m/s)
Low	0.96	1.07	1.02
Medium	1.21	1.39	1.30
High	1.52	1.70	1.61

Table 6. ESP Air Cleaner Flow Rates

Flow Setting	Specification cfm (m^3/s)	Measured cfm (m^3/s)	Relative Error (%)
Low	225 (0.106)	219 (0.103)	2.7
Medium	275 (0.130)	280 (0.132)	1.8
High	365 (0.172)	347 (0.164)	4.9

The velocity results obtained for the HEPA filter are shown in Figure 8 in the same format as above. Because the inlet and outlet flow areas are not the same in this model, no direct comparison can be made between the velocities at the inlet and outlet of this unit. It can be seen, however, that there is a large degree of variability in the flow velocities across the outlet of the unit. This is due to the unit design. The average velocities obtained separately for the inlet and outlet were used with the corresponding flow areas to calculate flow rates. The average between the inlet and outlet flow rates was taken to be the overall flow rate at each flow setting. Table 7 summarizes these flow measurement results. No specifications were provided by the manufacturer of the air cleaner for its flow rates, so no comparisons could be made.

Figure 8. Local Velocities of the HEPA Filter (top inlet, **bottom outlet**)

Local Velocity (m/s)										
High				Medium				Low		
1.07 **6.32**	1.05 **5.41**	0.88 **2.05**		0.82 **4.67**	0.69 **4.52**	0.72 **1.453**		0.71 **3.45**	0.59 **3.67**	0.60 **1.21**
1.01 **5.73**	0.82 **6.24**	0.84 **1.69**		0.82 **4.51**	0.62 **5.03**	0.72 **1.34**		0.68 **4.83**	0.49 **2.85**	0.56 **1.13**
1.17 **1.89**	0.82 **1.27**	0.98 **1.47**		0.86 **1.50**	0.64 **0.98**	0.78 **1.13**		0.76 **0.98**	0.53 **0.79**	0.62 **0.97**

Table 7. Flow Characteristics of the HEPA Filter

Flow Setting	Upstream Flow Rate cfm (m^3/s)	Downstream Flow Rate cfm (m^3/s)	Overall Flow Rate cfm (m^3/s)
Low	271 (0.128)	278 (0.131)	275 (0.130)
Medium	326 (0.154)	352 (0.166)	339 (0.160)
High	422 (0.199)	449 (0.212)	436 (0.206)

3.1.4.2 Filtration Efficiency - Inert Aerosol The single-pass testing of the air cleaners' filtration efficiencies was completed in two stages. The first stage covered the range of particles with diameters between 0.03 μm and 0.3 μm. The second stage covered the range from 0.3 μm to 10 μm. The results from the two stages were combined, and Figures 9 and 10 show the filtration efficiencies obtained for the air cleaners over the entire range of particle diameters. All efficiencies are plotted at the geometric mean of the measured size bin.

Figure 9. Filtration Efficiency for the ESP Air Cleaner

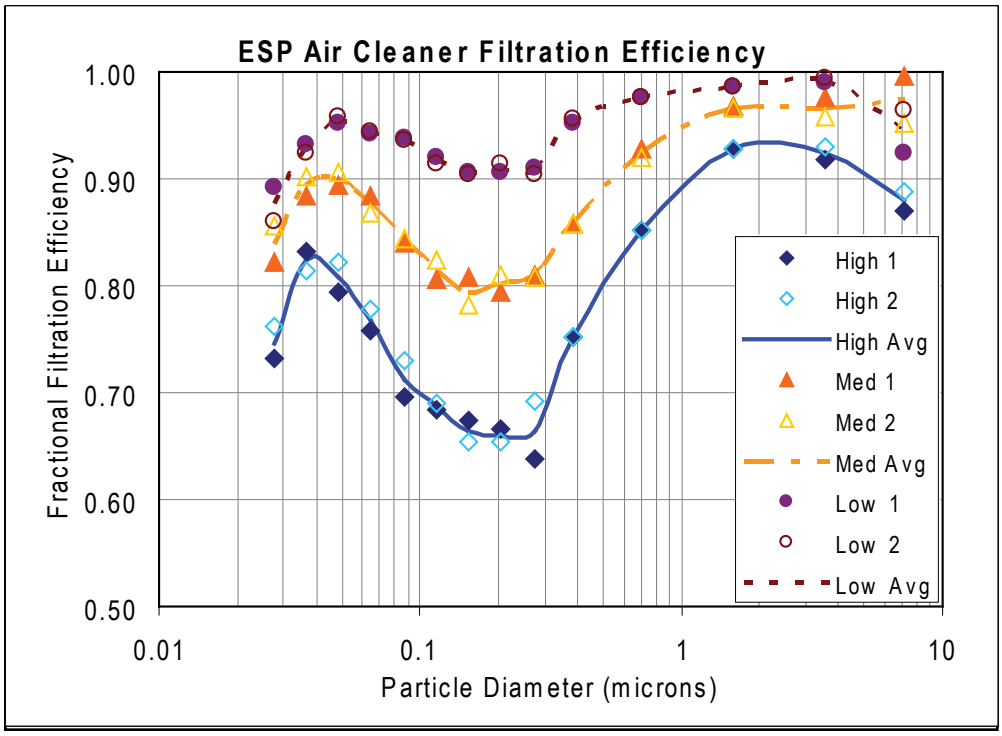

Figure 10. Filtration Efficiency for the HEPA Filter

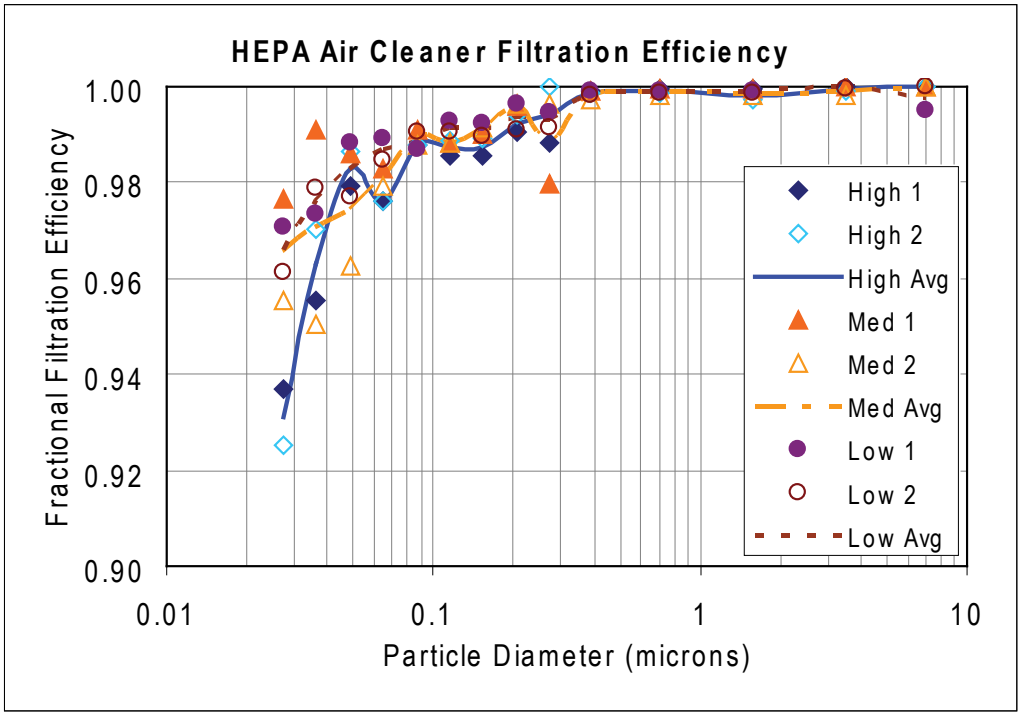

It can be observed from the two graphs that the filtration efficiency data obtained using two different aerosols and two different instruments show good agreement. The vertical red lines shown in the figures denote locations where the two branches of filtration efficiency curves are connected, for both air cleaners. Also, the graphs indicate good agreement between the duplicate runs performed for all test conditions. There was somewhat more data scatter observed for the smallest particles tested. This is mostly due to the lower concentration of these particles in the challenge aerosol and relatively high filtration efficiency of the air cleaners, which results in lower counts of these particles at the downstream location and, accordingly, leads to their poor counting statistics.

The results obtained for the electrostatic precipitator show that there is a minimum in the filtration efficiency curves, associated with particle diameters in the neighborhood of approximately 0.2 μm. This dip in efficiency is a well-recognized phenomenon for electrostatic precipitators; it is related to the two charging mechanisms present in such devices — field charging and diffusion charging. Field charging results from distortions in the electrical field lines, which are caused by particles greater than approximately one micron. These distortions cause charged ions traveling along the field lines to impact on the particle and charge it. Diffusion charging is dominant for particles less than approximately 0.1 microns. It results from random collisions between small particles and charged ions due to Brownian motion. Between 0.1 and 1 micron, neither mechanism is dominant and a minimum in collection efficiency is typically seen. Zukeran et al. cited observations of poor particle collection efficiencies of ultrafine particles (0.01–0.1μm) for electrostatic precipitators. They proposed poor charging and flow instabilities as possible causes for this observation.

It can also be seen in Figure 9 that there is a clear trend of increasing efficiency with decreasing flow rate for the electrostatic precipitator. This is a result of increasing particles' residence time within the unit at lower flow rates, which allows more time for their charging and transport to the collector surface.

The filtration efficiency curves obtained for the HEPA filter unit do not show any clear trend with respect to the flow rate. The data show that the efficiency decreases with particle diameter smaller than approximately 0.3 μm. For particles above 0.3 μm in diameter, however, the efficiencies were found to approach HEPA specifications. The cause for the unexpected but systematic decrease of filtration efficiency for particles smaller than 0.3 μm in diameter is not known at this point; it may simply be due to some leaks associated with relatively loose fitting of the filter media in the unit. It should also be noted that the particle-counting statistics from the SMPS were much poorer than from the Climet due to the instrument design and operating principle, even though it represents the state of the art in nanoparticle measurement. Nevertheless, the decrease in efficiency for smaller particles is also consistent with the CADR value decreasing from 330 cfm (0.156 m^3/s) for larger dust and pollen particles to 320 cfm (0.151 m^3/s) for smaller smoke particles, as shown earlier in Table 1.

It should also be noted that both air cleaners display the same significant drop-off in filtration efficiency for nanoparticles with diameters smaller than ~0.04 μm, the exact cause of which is also not known, especially for HEPA filters, and may represent an area of further investigation.

3.1.4.3 Filtration Efficiency- Bioaerosol During the single-pass testing of the air cleaners using bioaerosol, concentrations were measured with both the Climet CI-500 instrument and with water soluble gelatin filters. Three sets of filter samples were obtained for each air cleaner, simultaneously taking aerosol samples at the upstream and downstream locations of the test units. The Climet measurements were taken between each set of filter samples. The gelatin filters were sampled simultaneously for a predetermined period of time, each sampling at a 10 L/min flow rate. As specified in the test matrix, both air cleaners were tested at their medium flow rates only, and the results were compared to those obtained for the inert aerosol. Figures 11 and 12 show the results obtained from the bioaerosol testing for the ESP and HEPA filters, respectively. In these figures, the green line represents the average filtration efficiency observed using the Climet CI-500, and the yellow line represents the efficiency measured earlier during the inert aerosol testing. Good agreement is observed between these Climet CI-500 measurement results. The results from the gelatin filters are plotted in the graphs using the blue symbols, assuming that the microorganisms are detected as 1-μm particles, although, as mentioned above, the bacteria are actually elongated particles with approximate dimensions of (0.7–0.8) μm x (1.0–1.5) μm.

Figure 11. ESP Bioaerosol Filtration Efficiency

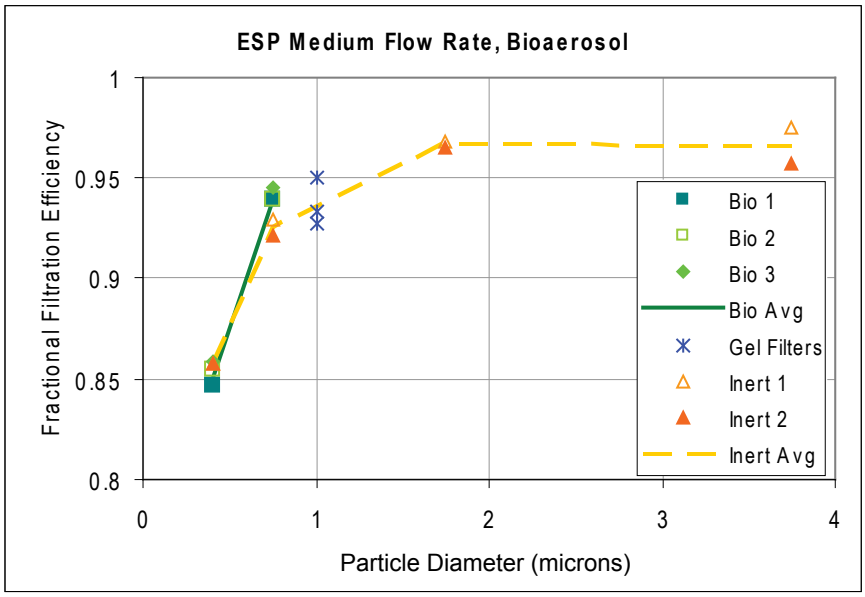

Figure 12. HEPA Bioaerosol Filtration Efficiency

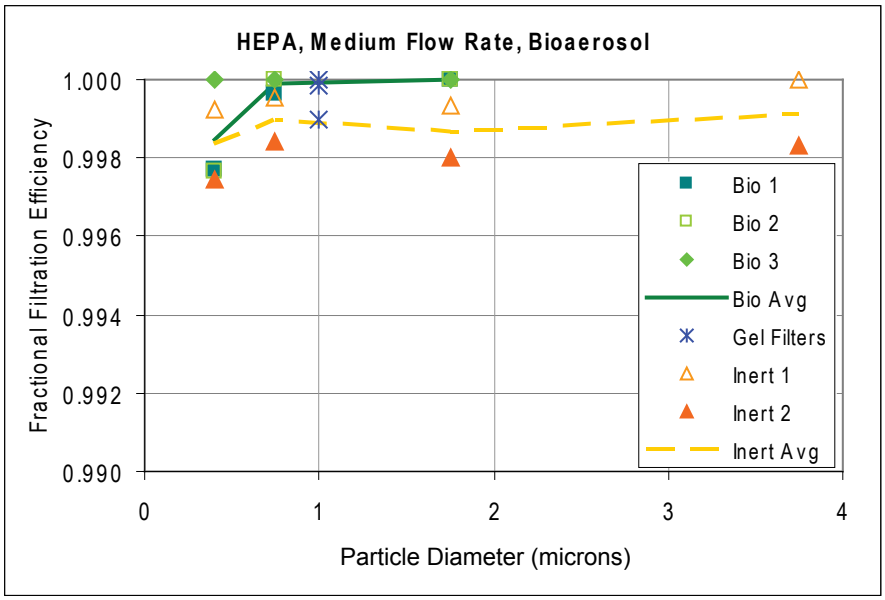

In Figure 11, Climet CI-500 measurements are plotted for the bioaerosol for only the first two particle size ranges of the instrument, since the downstream counts were too low for the larger particles with respect to the background counts to allow for accurate measurements. This is illustrated in Figure 13, which shows the downstream particle counts for the second run with the electrostatic precipitator, along with the corresponding background counts. It can be seen from this graph that the background is on the same order of magnitude as the measurements for the larger particles, indicating that the efficiencies calculated from those size bins cannot be considered accurate with any certainty. This was a problem unique to the bioaerosol tests due to the relatively low challenge concentration compared to the inert aerosol. Because of this, the gel filters were a more effective measurement of bioaerosol penetration.

Figure 14 shows the upstream particle counts obtained during the same run considered in Figure 13. From the graph no clear peak can be resolved in the size distribution of aerosol particles that can be identified with the airborne microorganisms. The lack of a peak is likely due to the impurities in the biological powder that was used to prepare the slurry. Therefore, an order-of-magnitude analysis was performed for the purpose of determining what portion of the challenge aerosol best represents the spores. It was determined, based upon the measured concentration of the initial slurry and the results obtained from the gelatin filters,

that the upstream spore counts should have been on the order of 7,000 to 10,000 during each run. Returning to Figure 14, it can be seen that particle counts obtained during this run for the 0.5 μm to 1 μm size bin are on the same order of magnitude as expected. Therefore, it was concluded that the efficiencies measured for the 0.5 to 1 μm size bin should give a close representation of the efficiency that can be expected for the biological particles, which also agrees well with the actual size of the spores as discussed above.

Returning to the efficiency curves shown in Figures 11 and 12, very strong agreement can be seen between the results obtained for both air cleaners using the biological and inert aerosols in the 0.5 to 1 μm size bin. Also, the efficiencies measured using the gelatin filters, which are plotted as blue symbols corresponding to the 1 μm particles, fit well to the curves obtained using the CI-500 particle counter. From the above analysis, it can be concluded that the performance of both units was consistent for both inert and biological aerosols.

Figure 13. Downstream Particle Counts From ESP Bioaerosol Test, Run 2

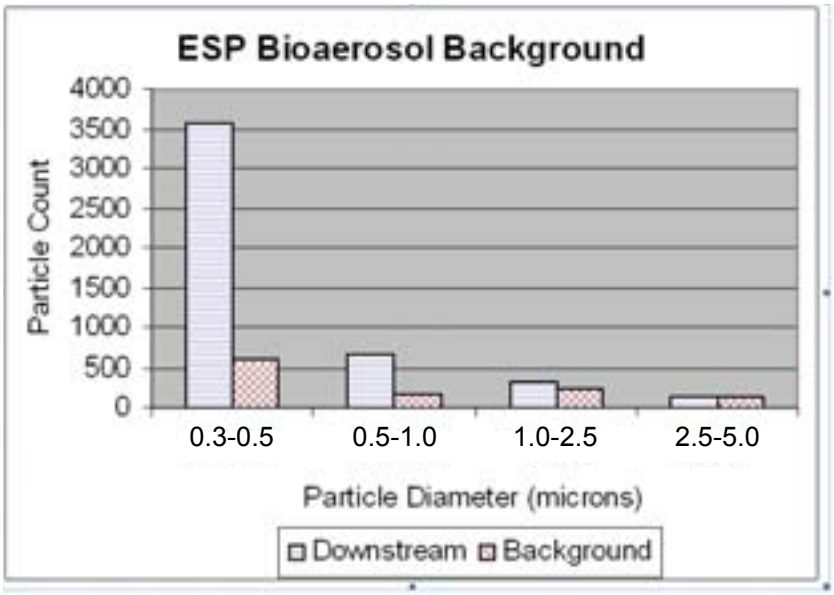

Figure 14. Upstream Particle Counts From ESP Bioaerosol Test, Run 2

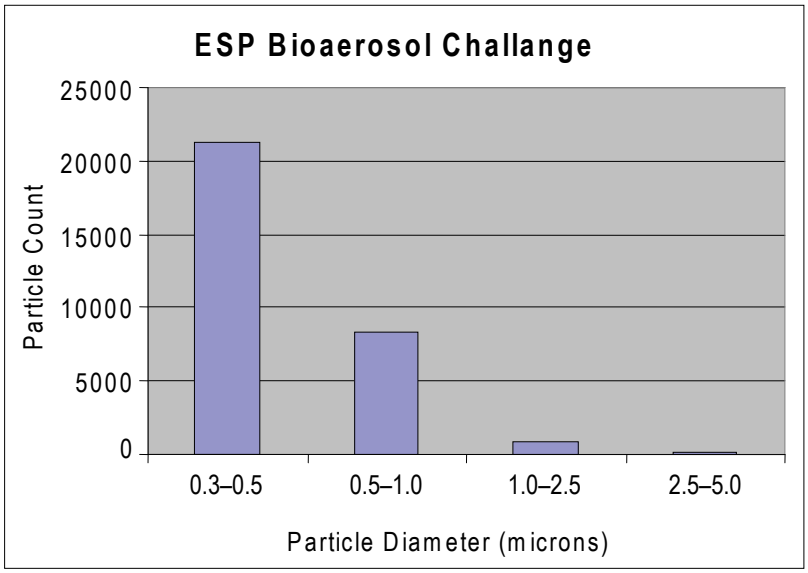

3.2 In-Room Testing of Air Cleaners

The purpose of the in-room testing was to investigate the effectiveness of a room air cleaner in an operational setting. There are two essential characteristics of a room cleaner that are independent of operational setting, i.e., its single-pass filtration efficiency and airflow capacity. However, the effectiveness of the air cleaner in removing airborne pollutants in a room is also dependent upon such characteristics as the flow pattern and degree of mixing that the air cleaner induces in the room. An air cleaner will not be effective if a flow patterns establishes in the room that causes a high level of clean air recirculation from its outflow back into the inlet. Based on the results of the single-pass testing, the HEPA filter was selected as a more efficient room air cleaner for testing.

In order to test the overall effectiveness of the air cleaner under particular operating conditions, concentration decay profiles were obtained by measuring aerosol concentration as a function of time within an enclosed chamber after generating a KCl aerosol. In addition, the degree of mixing in the chamber was assessed by collecting filter samples at several locations, which can be related to the variability of exposure dosages in the chamber and used as a measure of the mixing ability of the air cleaner.

3.2.1 Test Setup

The in-room testing took place in an 8 ft x 16 ft x 8 ft (2.4 m x 4.9 m x 2.4 m) chamber located at Battelle's West Jefferson facility. The chamber was sealed as tightly as possible with silicon caulking. The only air exchange with the surrounding room was diffusion through any remaining tiny cracks and four static HEPA filters installed in the walls to provide over-pressure relief. Two blowers were attached to the chamber to provide recirculation but were not used in this study. A photograph of the chamber is shown in Figure 15.

Figure 15. Test Chamber for In-Room Experiments

A KCl aerosol was generated within the chamber using a nebulizer similar to that used in the single-pass testing. The concentration within the chamber was measured continuously using the Climet CI-500 laser particle counter. A total of five open-face filters were used during each test. The filters were used to simulate the cumulative exposure levels of theoretical occupants during the test period at the five strategic locations within the chamber. They also provided a method for characterizing the mixing conditions within the chamber. The test matrix developed for the in-room testing is summarized in Table 8.

Table 8. In-Room Test Matrix

Type of Aerosol	Location of Source	Location of Air Cleaner	Air Cleaner Capacity	Number of Tests	Configuration Code
Inert aerosol (0.3 to 10 μm)	Center	No air cleaner	Zero	2	D
		Near source	High	2	A
	Near wall	Remote from source	High	2	B
		Remote from source (Desk)	Low	2	C

Figures 16 through 18 show the three principal setup configurations used in this testing (Configuration D is the same as Configuration A but with the air cleaner not operating). All the sampling locations were fixed in the chamber, while locations of the air cleaner and the nebulizer were varied. The Climet CI-500 laser particle counter was placed in the middle of the chamber at a height of approximately 5.5 feet (1.7 m). One open-face filter was placed next to the CI-500 at the same height. The remaining four filters were placed approximately one foot from the walls in each of the four corners. The heights of these filters were alternated between 5.5 feet (1.7 m) and 3.5 feet (1.1 m), as shown in the diagrams. The two heights were chosen to represent a person standing and sitting.

Simple calculations were performed to determine an appropriate aerosol generation rate for the measurements. The manufacturer of the Climet CI-500 specifies an upper limit to aerosol concentration of 10^7 particles per cubic foot (~350 particles/cm^3). However, a sufficient aerosol concentration must be present in the chamber to allow a quantifiable mass to be collected on the filters. The most accurate balance available for this project could record up to six significant digits, i.e., up to 1 microgram. In order to minimize any measurement error, collecting a mass on the order of hundreds to thousands of micrograms was desired.

Figure 16. In-Room Test Configuration A

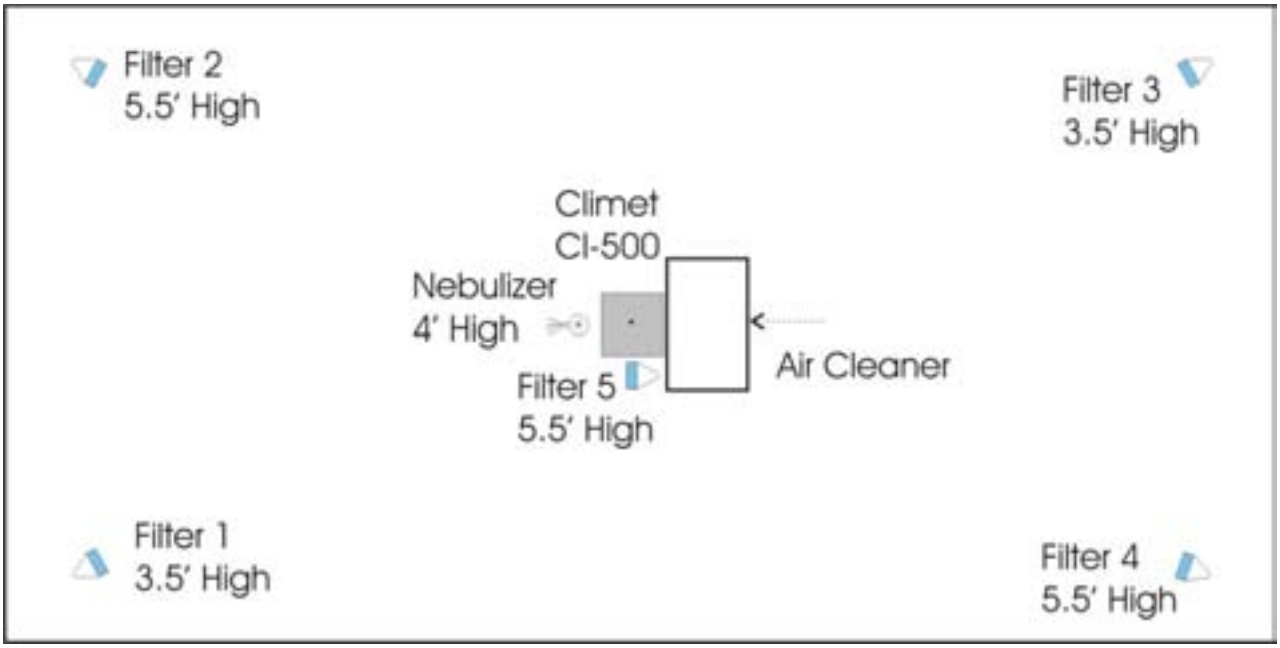

Figure 17. In-Room Test Configuration B

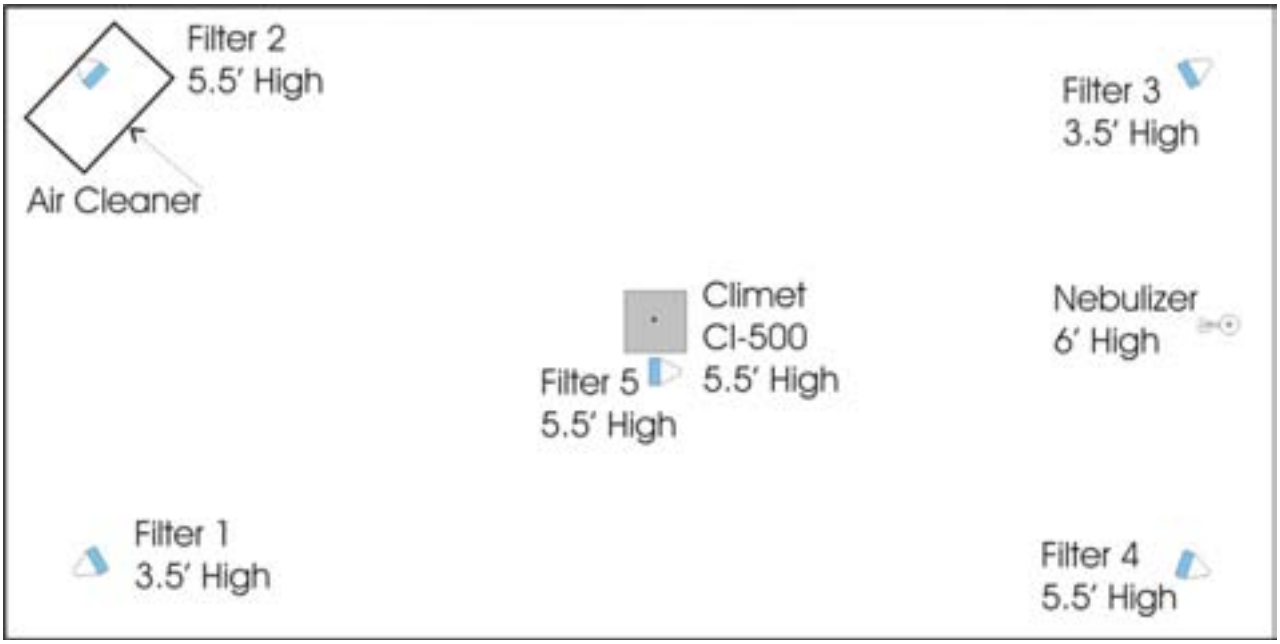

Figure 18. In-Room Test Configuration C

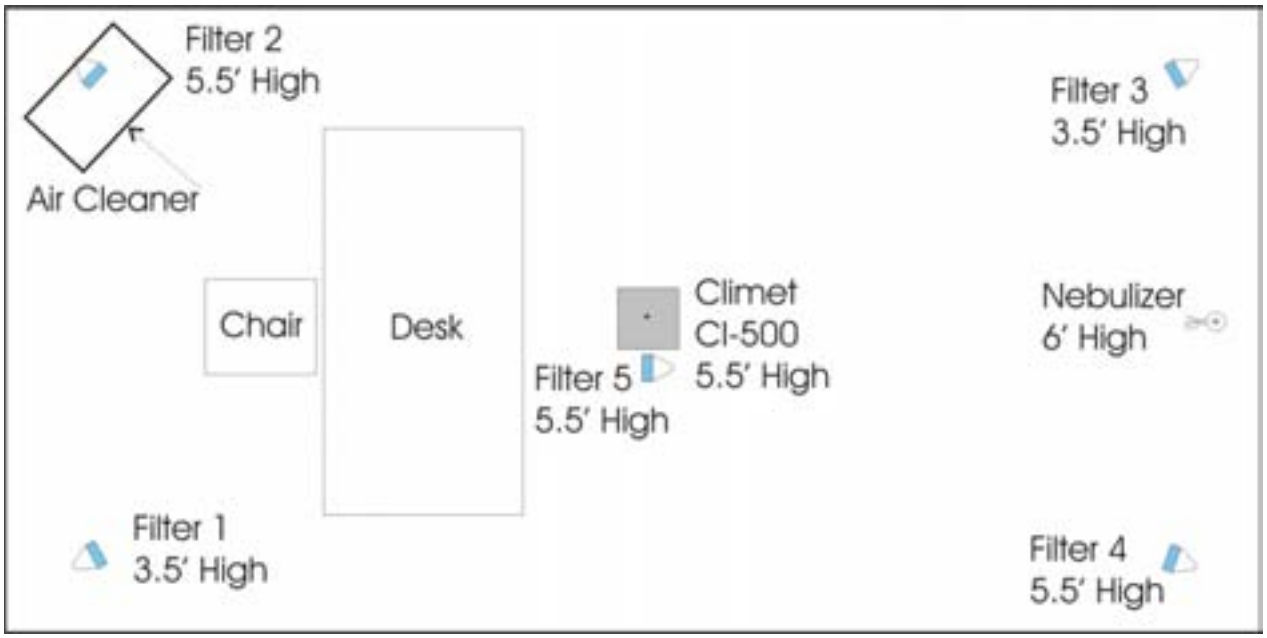

It was estimated that the mass collected on the filters would be on the order of only tens of micrograms if aerosol concentration was maintained in the chamber within the CI-500 detection limit, assuming a constant concentration of 10^7 particles per cubic foot, 0.3 micron particle diameter, and 10 L/min sampling flow rate for 30 min. Considering also that the concentration would be lower at some sampling locations, and decreasing in time, it was determined that it was not desirable to run both the Climet and the filter samplers under the same conditions.

Thus, two separate nebulizers were used to achieve the required concentrations in the test chamber, and the tests were performed in two stages. During the first stage, a low concentration aerosol was generated and real-time concentration measurements were performed using the Climet. During the second stage, a higher aerosol concentration was achieved under otherwise similar conditions, and the filter samples were collected. Climet measurements were also taken during the second phase, but any readings that exceeded the detection limit of the instrument were considered invalid. Both stages of the test were performed without changing the test configuration.

3.2.2 Test Procedure

As described above, the in-room tests were performed in two stages. The procedure for these tests was as follows. At the beginning of the test, the background within the chamber was brought down to a level of no more than 10^5 particles per cubic foot (i.e., not to exceed 1% of Climet CI-500 max concentration limit). This was done, using a second in-room air cleaner (used in the single-pass efficiency testing), because preliminary testing showed that the chamber ventilation system was not effective in decreasing the background aerosol to the desired concentration level.

After the desired background was achieved, the auxiliary air cleaner was turned off and the test air cleaner turned on. At this point (time zero) the low concentration nebulizer was switched on. The nebulizer was run for 10 minutes, after which it was turned off, while the air cleaner continued running. This stage of the test was considered complete when the concentration was returned to the background level or after one hour (which only occurred in the tests configured with no air cleaner running). In the latter case, the auxiliary air cleaner was then used to return to the background level.

The second stage of the test began once the background concentration was achieved. This stage was run similarly to the first stage with respect to the test configuration. At the beginning of stage two, the filter sampling pumps and the high concentration nebulizer were simultaneously turned on. The nebulizer was run for 10 minutes, after which it was turned off, while the filter sampling pumps and the air cleaner continued running for another 50 minutes. A constant time of one hour was selected for running the sample filters to allow for dosage comparisons between the different test configurations.

It should be noted that the air cleaners were running throughout the test, including during the aerosol generation period, in order to simulate a realistic attack scenario. In such a scenario, the air cleaner would be running continuously and would offer some protection during as well as after the release. This also allowed for some assessment of how well the air cleaner mixed the air within the chamber and for assessing the effect of room configuration on the performance of the air cleaner.

3.2.3 Data Analysis

For each in-room test configuration, two principal data sets were obtained, real-time concentration data from the Climet, which was used to construct concentration vs. time profiles, and the cumulative exposure data obtained using sample filters. The concentration vs. time plots were used to illustrate the mitigation capabilities of the air cleaner.

The total decay constant, "k", characterizes the rate at which particles are removed particles from the air in the chamber; it combines both the effect of the air cleaner and deposition within the chamber. Due to the small size of the particles generated in this study, deposition is assumed to have a minor effect on the measured value of k. "K" is therefore indicative of the air cleaner effectiveness. "K" was determined by fitting an exponential function, Equation 4, to the data points between the peak concentration (C_0) and the point when the concentration dropped to less than two times the background.

$$C = C_o e^{-kt} \quad (4)$$

Where:

C = aerosol concentration at time t, particles/ft^3 (particles/m^3),

Co = peak aerosol concentration, particles/ft^3 (particles/m^3),

k = overall rate constant of concentration decay, 1/min (1/s), and

t = time, min (s).

The second set of data consists of the five open-face filter samples. All filters were run for one hour as discussed above. In addition to assessing the effect of an air cleaner on the cumulative exposure level, comparing the mass collected on each of the five filters from the same run allowed for a characterization of the mixing within the chamber. This can be illustrated by calculating the CV for the five sampling locations.

3.2.4 Results and Discussion

3.2.4.1 Decay Rate For each test configuration, the real-time concentration vs. time results are plotted in Figure 19. In addition, Figure 20 shows the configuration-average profiles determined for each of the test Configurations A, B, and C.

Figures 19 and 20 show graphs of total particle number concentrations plotted as functions of time. Since particle deposition rate in the chamber is also dependent on particle diameter, Figure 21 shows particle number concentrations plotted as functions of time for the six particle diameter bins of the Climet CI-500 instrument used in the study. The particle concentrations in Figure 21 were normalized by the respective peak concentrations of the size bins in order to illustrate the relative decay rate for the different particle sizes. According to this figure, some increase can be seen in the decay rate with increasing particle diameter. The decay constants calculated from this plot ranged from 0.315 for the smallest particles to 0.398 for the largest particles. Based upon the results of the single-pass efficiency measurements, which showed high filtration efficiency values for particles between 0.3 and 10 microns, the difference in decay constants is attributed to the increased settling velocity of the larger particles.

Concentration decay constants were determined for each of the curves shown in Figure 19. The total particle concentration was chosen for determination of *k*, instead of size-dependent decay, for ease in comparing the various test configurations. These constants were calculated by fitting exponential functions to the data points obtained for each curve between the peak concentration and the point when the concentration decreased to less than two times the initial background level. The average *k* values were then determined for each of the test configurations, which are shown in Table 9. The R^2 value for the fit of all the curves was greater than 0.99, indicating a very good fit to Equation 4.

Figure 19. Concentration vs. Time Plots, Individual Configurations

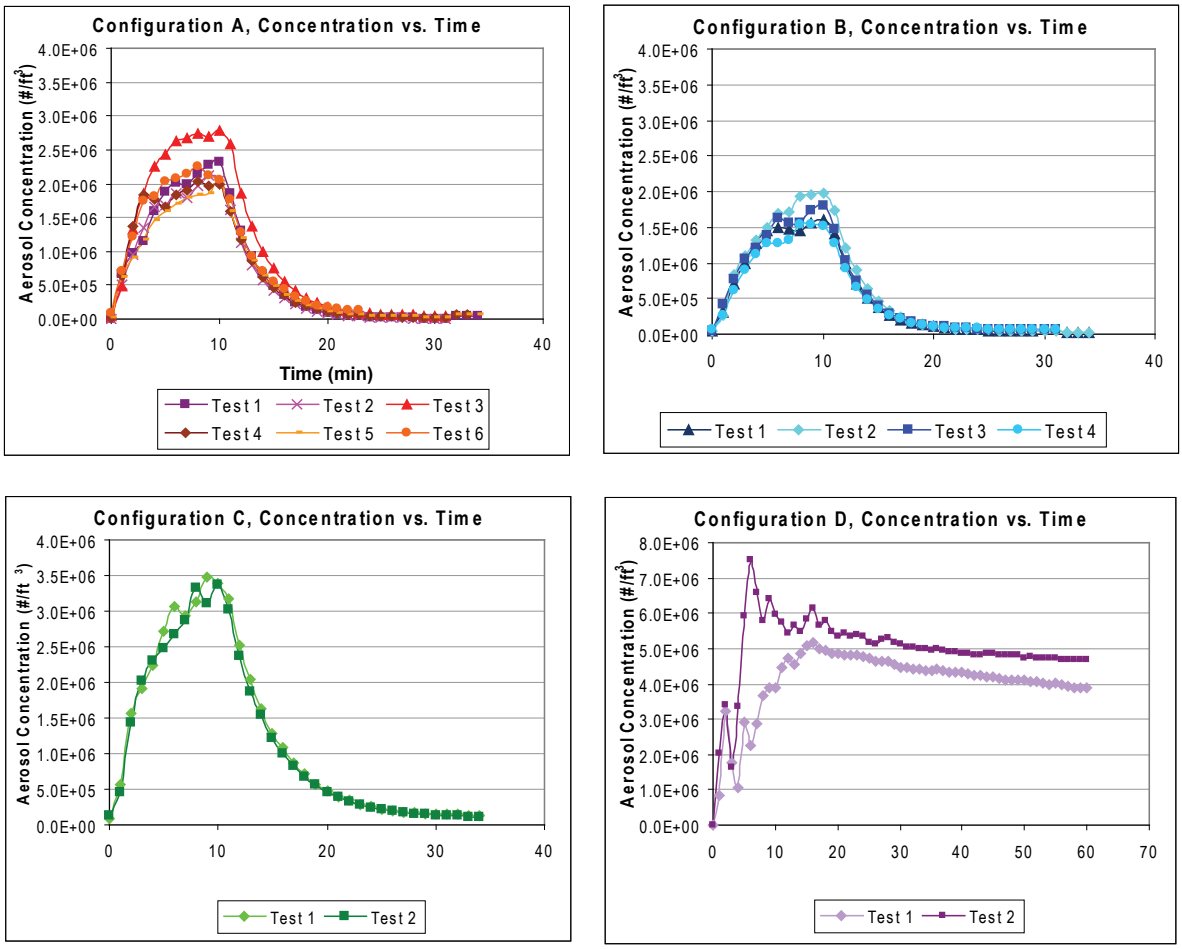

Figure 20. Concentration vs. Time Plot, Averaged Data

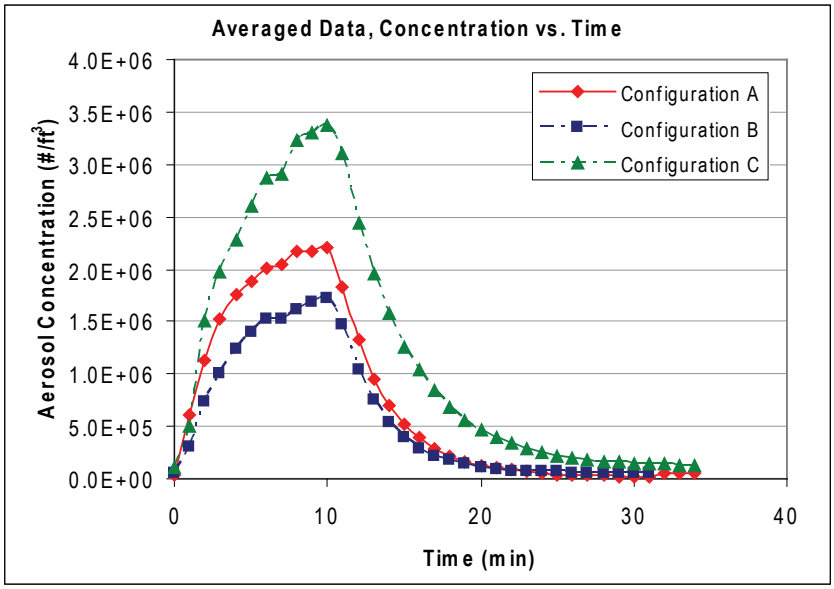

Figure 21. Size Resolved Concentration vs. Time

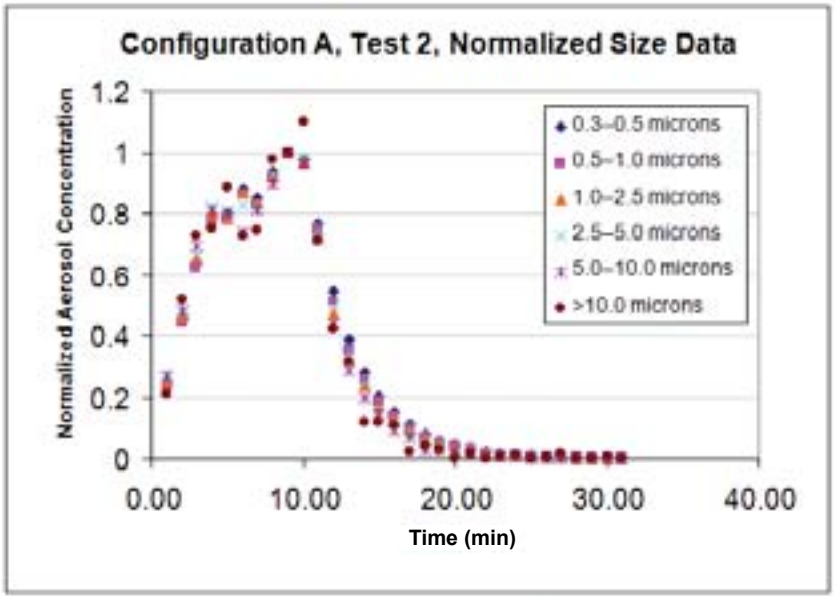

Table 9. Calculated Decay Constants (1/min)

Run #	Scenario A	Scenario B	Scenario C	Scenario D
1	.318	.285	.188	.0058
2	.316	.296	.191	.0055
3	.275	.286	No test performed	No test performed
4	.283	.283	No test performed	No test performed
5	.279	No test performed	No test performed	No test performed
6	.262	No test performed	No test performed	No test performed
Average	**.289**	**.287**	**.189**	**.0057**

The chamber tests were run in series, with different scenarios tested at different times. There were a total of six tests performed in Configuration A, as additional Configuration A tests were run during each test day to ensure that consistent conditions were used in all trials. As shown in Figure 19, the variability in the aerosol test conditions maintained during subsequent tests in the same configuration was low. Considering the decay constants in Table 9, however, some variability was observed in their individual values calculated for Scenario A. Runs 1 and 2 were performed during the first test period, Runs 3–5 were performed during the second test period, and Run 6 was performed during the final test period. The decreasing decay constant was attributed to the increasing leak of ambient particles into the chamber, caused by its expansion and contraction over the summer test period, as suggested by the gradually increasing level of achievable background counts. Simple "well-mixed model" calculations were also performed, which also suggested that this could account for the slight decrease in the observed decay constant for test Configuration A. Nevertheless, the background never exceeded 5% of the peak aerosol concentration in this testing, and the CV in the decay constant was on the order of 6%.

A number of observations can be made from these data. The most obvious observation is that the concentration within the chamber decayed much more slowly when the air cleaner was not turned on (Configuration D), indicating that the presence of the air cleaner had a significant mitigating effect. As expected, there also was a clear increase in the mitigation ability of the air cleaner with increasing flow rate, which can be seen by comparing the decay constant determined for Configuration C to those of Configurations A and B.

It can also be observed from both these plots and the calculated decay constants for Configurations A and B that no significant difference was observed in the performance of the air cleaner in these different test settings. In Configuration B, when the air cleaner was positioned farther from the nebulizer, it may have been slightly more effective than in Configuration A. This may be due to the fact that in Configuration B the nebulizer was pointed in the direction of the air cleaner inlet, whereas in Scenario A the nebulizer was pointed in the opposite direction. When the nebulizer is pointed in the direction of the air cleaner inlet, the flow of aerosol toward it is enhanced in comparison with the nebulizer pointing in the opposite direction. This effect is

the likely explanation for the higher peak concentration of aerosol observed at the Climet location for Configuration A than for Configuration B. However, the decay constants were very similar for both cases, indicating that after some adequate mixing time, the effectiveness of the air cleaner was practically equivalent between these two configurations.

3.2.4.2 Mixing Efficiency and Dosage In addition to the real-time monitoring of aerosol concentration in the test chamber, cumulative samples of aerosol were collected using standard 47-mm filters for each of the four test configuration. Average mass and CV between the different filter locations were calculated. A summary of the results is shown in Table 10, and the individual filter masses are graphed in Figure 22. The average mass values can be compared between different test configurations to give a relative exposure dosage received in the room over a one-hour period. The CV gives a relative indication of the mixing conditions developed within the chamber.

As expected, the masses collected on the individual filters varied to some extent between Configurations A and B; however, the average mass collected and the CV were found to be very close. This supports the conclusions made from the concentration decay data that, although the flow patterns within the chamber were different between these two test configurations, the air cleaner induced sufficiently high mixing conditions in both cases to result in an overall similar effectiveness of the air cleaner.

The dosage observed in Configuration D (air cleaner not operating) was found to be more than an order of magnitude greater than those obtained for Configurations A and B, indicating a significant protection factor provided by the air cleaner. Also, the CV in Configuration D was much higher, indicating a much slower mixing process.

For test Configuration C (low flow setting, desk in the room), the dosage was higher than in Configurations A and B, as expected, due to the lower concentration decay rate. However, according to the CV values, no decrease in the mixing efficiency was observed in this case.

Table 10. Collected Filter Masses

Test	Average Mass (μg)	CV
Scenario A 1	667	35%
Scenario A 2	550	17%
Scenario B 1	564	28%
Scenario C 1	1086	19%
Scenario C 2	989	18%
Scenario D 1	7571	42%

The variability in the filter masses collected at different sampling locations, observed during the in-room testing of the air cleaner, is also illustrated as a diagram in Figure 22. This diagram shows that despite the fact that the air cleaner has high airflow capacity, relative to the size of the test room, the level of mixing it induces, although high, is not "perfect" (referring to the perfectly-mixed zone concept frequently used in model calculations). In fact, while the air cleaner promotes convective mixing in the room, it also creates and maintains a low-concentration zone in its outflow region, as well as a point of very high aerosol concentration at the aerosol source during generation. Therefore, the effectiveness of a room air cleaner in mitigating the effect of an aerosolized agent attack on a building will strongly depend upon the agent dissemination scenario. Nevertheless, based on the results of this investigation, it can be concluded that a room air cleaner may lead to a very significant reduction in the level of indoor exposure to the agent, which may be approximately evaluated using the well-mixed zone concept.

Figure 22. Collected Filter Masses

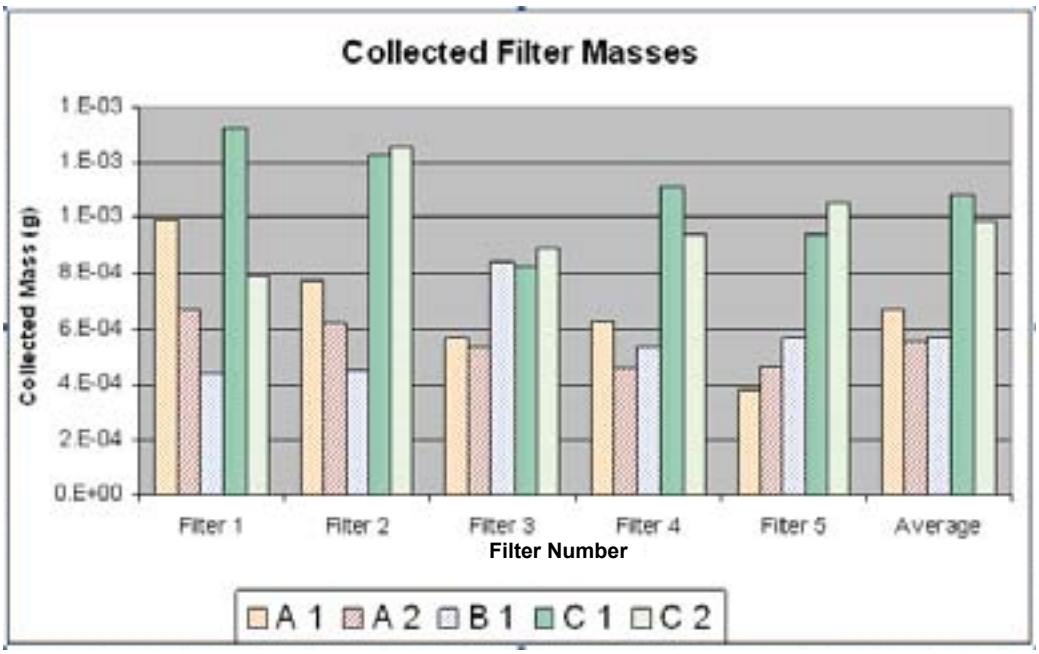

4.0
Modeling Study

Mathematical modeling is widely used in countless applications, especially when experimental investigations are impractical for one reason or another (for example, cost of experimental trials may be prohibitively high). In the context of this work, as mentioned above, the effectiveness of an indoor air filtration system against an aerosolized agent attack on a building is highly scenario-dependent, and its detailed exploration would require considering a great number of cases. A computational fluid dynamics (CFD) model was therefore used in this project with the purpose of evaluating the accuracy and efficiency with which it can predict concentration evolution of contaminant in the room air. A CFD package, FLUENT, was used to implement the model and generate the numerical simulations. The model geometry and flow conditions selected represented Configuration A of the in-room test scenarios discussed above. In addition, simplified calculations were performed based upon the perfectly-mixed zone assumption. This model was implemented in Microsoft Excel™, and the calculations were compared to the CFD model predictions and experimental results.

The ultimate goal of this task was to gain an understanding of how to correctly develop and use computational models to assess the effectiveness of an in-room air cleaner or other HVAC equipment in minimizing the impact of an agent dissemination attack on a building. There are two principal effects that an indoor air cleaner may have on the evolution of pollutant concentration in a room: enhanced mixing of the room air and cleaning the air by some aerosol removal mechanism. Both of these effects will result in the development of a unique scenario-, time-, and space-dependent concentration profile in the room of interest. The cost associated with testing all the potentially viable HVAC configurations would be prohibitive and logistically complex. Modeling, if properly applied, offers potential savings in identifying the main phenomena that control the effectiveness of in-room air cleaners in reducing the impact of an aerosolized agent dissemination event.

4.1 FLUENT CFD Modeling

A single simulation was performed under this task, using commercially available software to resolve the effect of air cleaner location on its effectiveness, addressing both the mixing and filtration aspects of the overall effect. Consideration of both these aspects is important because while air filtration acts to reduce pollutant concentration in a room, mixing tends to decrease a pollutant's spatial nonuniformity in the room, thus reducing its concentration at some locations while increasing it at others.

The CFD modeling approach was based on the Eulerian treatment, whereby the contaminant is treated as a continuum fluid dispersing in the air by advection and diffusion processes. The model geometry consisted of a rectangular room with a single air cleaner located near the center of the room, a nebulizer injecting an airborne challenge simulant for a portion of the simulation, one real-time aerosol concentration monitor, and five individual points for predicting the cumulative mass collected on the filter samples. The indoor air cleaner was treated as a stand-alone interior unit with specified dimensions, flow capacity, and contaminant removal efficiency.

The computer code FLUENT, a well-validated industry standard code for CFD calculations, was applied in this analysis. Using the model geometry and the boundary conditions, a steady-state three-dimensional solution was obtained for the in-room flow pattern, which was subsequently used to predict a time-dependent contaminant concentration field in the room. A highly resolved spatial and temporal map of the contaminant concentration profile was obtained and compared to experimental data. A more detailed discussion on the modeling approach and results can be found in Appendix B. A detailed description of the mathematical approach to CFD is available in the FLUENT User's Guide, which can be accessed online at FLUENT's Online Support Resources (FLUENT, 2007).

4.1.1 Results

From the CFD model calculations, aerosol concentration at each time step was determined at the locations of each of the five filter samples and the Climet, as used in the experiments. From these data, concentration vs. time plots were obtained, decay constants calculated, and the cumulative concentration was determined for each of the filter locations. The concentration vs. time curves predicted for each of the sample locations are shown in Figure 23. The decay constants were very similar for each of these curves, so the average was taken. The average decay constant for the CFD model was then found to be 0.535 1/min, which is much higher than that obtained from the experimental results (0.318 1/min).

As mentioned above, by integrating the curves in Figure 23, masses of aerosol particles collected on the simulated filters, or simulated exposure dosages, were determined and compared to the experimental results. In general, the predicted dosages were found for all locations to be somewhat higher than the experimental dosages, although the overall trends were captured. One of the reasons for this disagreement was associated with the uncertainty in the rate at which aerosol was introduced into the room. Since the experimental spray rate was not well known (the spray rate used in the model was based on an estimate obtained from a nebulizer characterization test spraying pure water), the masses from the CFD model predictions were normalized to give the same average filter mass as in the experiment, which was done for the results comparison purposes.

Figure 24 shows both the normalized and nonnormalized masses, predicted from the CFD calculations, as well as the average of the two experimental runs performed for this test configuration. The CV for the model filters is 23%, which is within the range of the experimental CVs shown in Table 10. As a result of this analysis, the CFD model appears to offer a reasonable potential for replicating the general trend of the experimental results, with the possible exception of Filter 5.

Figure 23. CFD Model Results

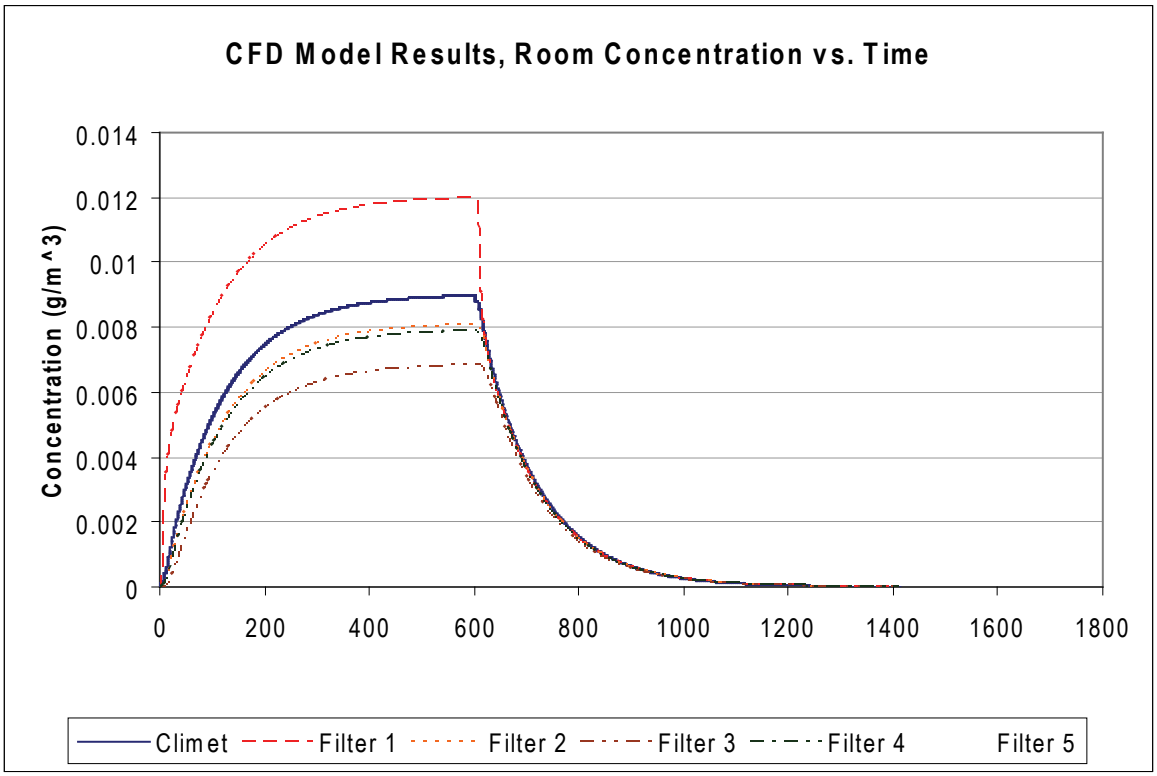

Figure 24. Filter Masses from CFD Calculations

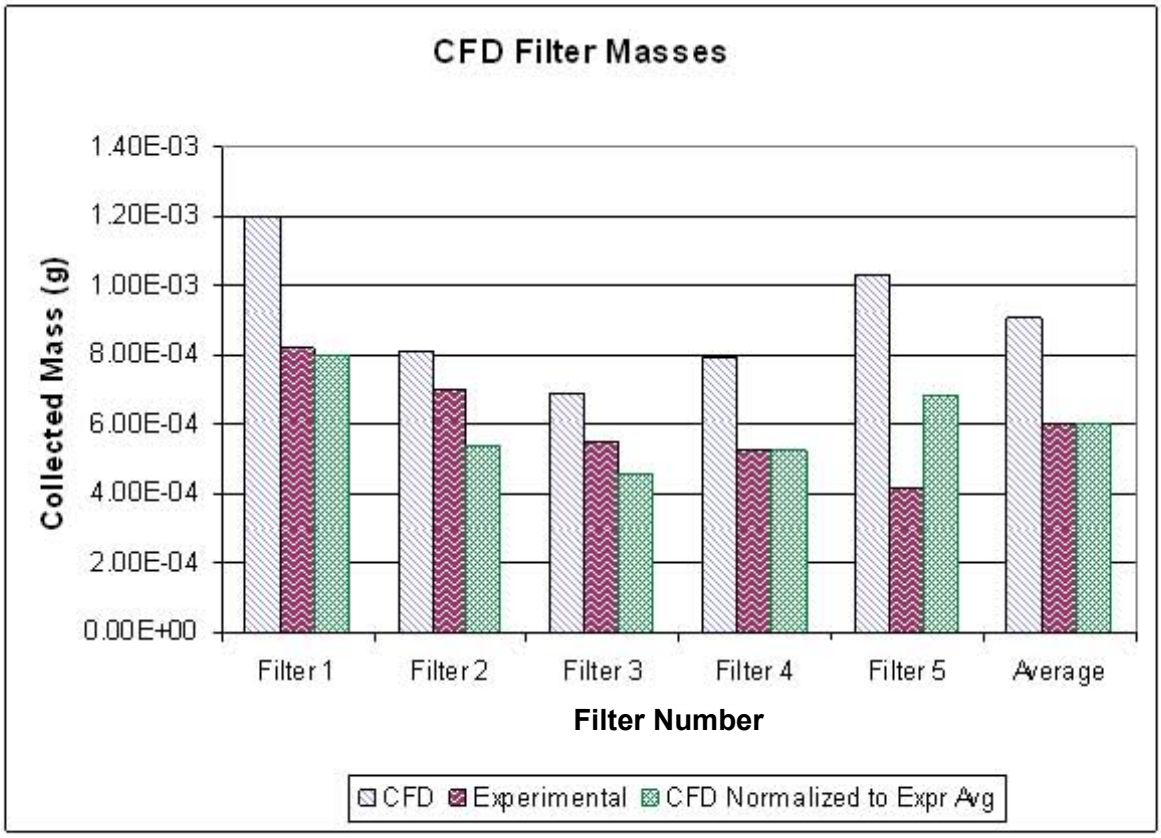

4.2 Perfectly-Mixed Zone Analysis

For comparison purposes, a series of calculations was also performed based upon the assumption that the chamber was instantaneously and perfectly mixed. The exact model is shown by Equation 5 (note an alternative derivation of the equation using SI units is shown in parentheses and would lead to *k* in units of 1/s). These calculations assumed that 100% of the particles that entered the filter unit were removed from the air and that deposition was insignificant. The calculations were performed using both the experimentally measured flow rate of the air cleaner, 450 cfm (0.212 m^3/s), and the certified clean air delivery rate (CADR), 330 cfm (0.156 m^3/s). The spray rate, expressed in particles/min, used in the calculations was determined by extrapolating back the decay curves obtained during the Configuration D tests (air cleaner not operating) to time zero. Figure 25 shows the results of these calculations plotted along with the test data obtained in one of the experimental runs. The decay constants are also shown on the graph, according to which their values obtained using the well-mixed zone calculations are appreciably higher than those obtained using the CADR value, and both are higher than the experimental value.

$$V\frac{dC}{dt} = \dot{N}_{spray} - Q_{filter} \cdot C \qquad (5)$$

Where:

V = the volume of the chamber, ft^3 (m^3),

C = the particle concentration, particles/ft^3 (particles/m^3),

$\dot{N}_{spray}$ = the spray rate, particles/min (particles/s), and

Q_{filter} = the flow rate of the air cleaner, cfm (m^3/s).

The CADR is determined experimentally, according to the AHAM procedure, reflecting the flow rate and filtration efficiency of the air cleaner, as well as its contribution to the degree of mixing established in the CADR test chamber. It is determined by measuring the concentration decay in an isolated test chamber that has been uniformly mixed prior to the test. Also, the air cleaners are rated for CADR using a test chamber smaller than that used in this study; besides, in this work, the challenge aerosol was not mixed prior to testing. Therefore, it was not unexpected that the HEPA filter would demonstrate a lower concentration decay rate during this testing as compared to the decay rate based on the CADR value.

Figure 25. Well-Mixed Zone Model Results

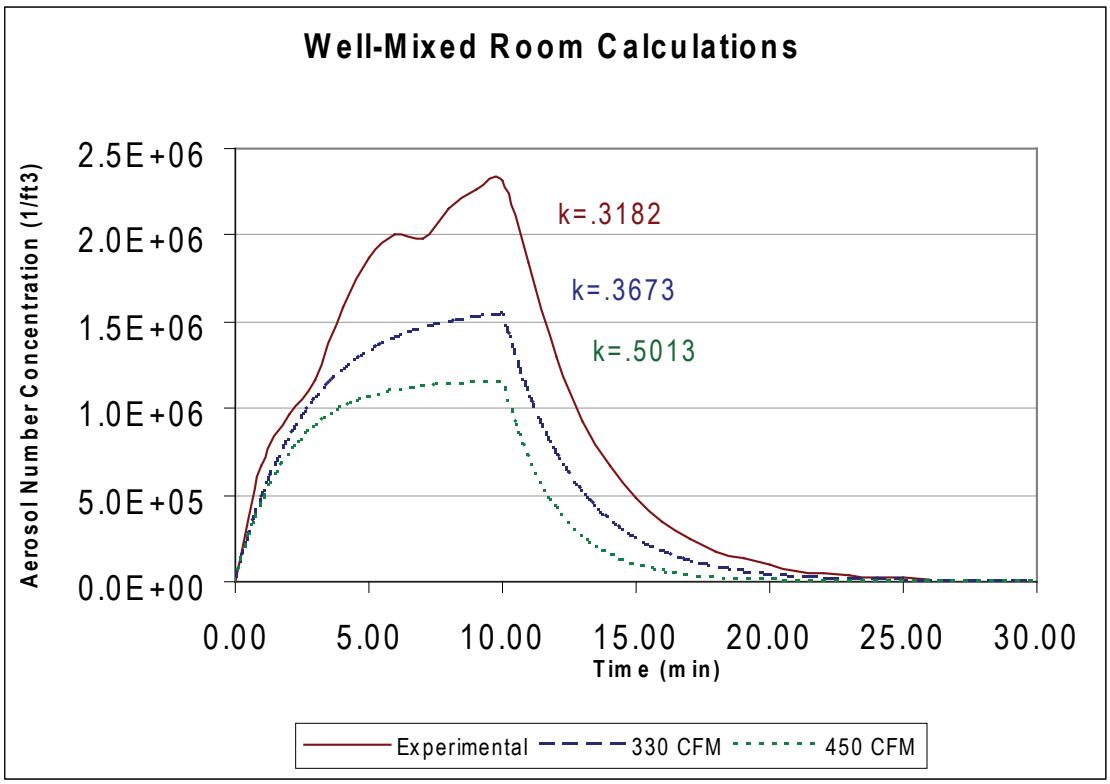

5.0 Conclusions

This report describes the investigations conducted to quantitatively verify the ability of room air cleaners (specifically, filters that remove PM) to mitigate the effect of an aerosolized biological agent attack on a building. Two filter systems were evaluated with regard to their building protection effectiveness. One of the air cleaners selected for this project used HEPA filtration technology, and the other was based on the principle of electrostatic precipitation. This work comprised both an experimental investigation and a modeling study.

The test air cleaners were experimentally evaluated for their single-pass filtration efficiencies as a function of particle diameter (ranging from 0.03 μm to 10 μm) and airflow rates, using both an inert aerosol and a bioaerosol. The HEPA filter was then selected for further evaluation, in a test chamber under various room configurations, to verify its effectiveness in reducing ambient levels of PM. In the test chamber experiments, the in-room particle concentration decay rate was determined from data obtained for a particular location in the chamber using a real-time particle counter.

Following the completion of the experimental phase of the project, model calculations were performed using computational fluid dynamics for one of the specific in-room test configurations. In addition, simple calculations were performed for the test conditions using the perfectly-mixed zone modeling approach.

During the single-pass efficiency testing, two replicate test runs were performed for each test condition to demonstrate the precision between them. The ESP-based air cleaner displayed a pronounced minimum in filtration efficiency for particles of ~ 0.2 μm diameter, which is consistent with the principles of electrostatic precipitation. Also, the single-pass efficiency of the ESP air cleaner was found to decrease with increasing flow rate through the unit, due to the decreasing residence time of the particles in the charging and deposition zones of the collector.

For the HEPA filter, no noticeable effect of flow rate on the filtration efficiency of the unit was observed, but an unexpected drop-off in efficiency was observed for particles below 0.3 μm in diameter. This observation could be explained by some leaks that probably developed aroundthe filter because of its relatively loose fit in the single-pass test unit. However, the consistent tendency of both air cleaners to have reduced efficiency for particles with diameters smaller than 0.04 μm warrants further investigation. No difference was observed between the air cleaners' filtration efficiencies for biological and inert aerosols having similar particle diameters.

The effectiveness of an in-room air cleaner in reducing a room's aerosol level under typical operating settings depends on three principal characteristics: 1) single-pass filtration efficiency, 2) filtration airflow rate, and 3) the airflow pattern that the cleaner induces in the room. While the first two characteristics can be obtained from some straightforward measurements, such as those used in this study, the airflow pattern in the room is also dependent upon such other factors as room size and shape, HVAC characteristics, furnishing, leak patterns, presence of mixing fans, etc. Some of these factors were investigated in this project using the HEPA filter. The HEPA filter was found to provide significant protection (in terms of reduced in-room air PM concentration) when compared to the case when the air cleaner was not operating. This observation was not unexpected and illustrates the potential usefulness of in-room air cleaners in the event of an aerosolized biological agent attack on a building. The location of the air cleaner relative to the aerosol source was found to have a minimal effect on reducing the PM level. The addition of an office desk and a chair in the test chamber also did not appear to noticeably alter the performance of the air cleaner. Overall, the HEPA filter provided reasonable mixing conditions in the test room, although some variability in the PM levels was observed for different locations inside the chamber.

The CFD model simulations performed under this study demonstrate the ability of this technique to predict aerosol levels in various indoor settings, with the caveat that it overestimated the PM concentration decay rate. The main issue associated with this application of CFD is the broad spectrum of flow regimes evolving within the room, ranging from laminar to fully turbulent conditions. This requires specification of different turbulence closure models, such as large eddy simulation for describing large flow recirculation patterns, and more refined schemes for considering the dispersion of contaminant in the aerosol generation and air cleaner "jet" exhaust zones. Depending on the particular scenarios of interest, CFD simulations can also be expensive to perform. In this regard, it is also recommended that an alternative modeling methodology be developed for evaluating the effectiveness of in-room air cleaners in real situations; this type of model would be capable of applying the CADR-type of characteristics to various room configurations while accounting for the different degrees of mixing the air cleaner may induce under different settings.

6.0
References

Association of Home Appliance Manufacturers. *Directory of Certified Room Air Cleaners.* Edition No. 3, 2004.

Association of Home Appliance Manufacturers. Method for Measuring Performance of Portable Household Electric Cord-Connected Room Air Cleaners. ANSI/AHAM AC-1-2002.

Association of Home Appliance Manufacturers. *Directory of Certified Room Air Cleaners.* Edition No. 3, 2005.

Consumer Reports. Air Cleaners, CR Quick Recommendations. (October, 2003).

FLUENT Online Support Resources. https://secure.fluent.com/sso2/login.htm (6/20/2007).

FLUENT User's Guide. Lebanon, NH, 2005.

Pope, S.B. *Turbulent Flows.* Cambridge University Press, 2000.

Reid, R.C., J.M. Prausnitz, and B.E. Poling. *The Properties of Gases & Liquids.* 4th Edition. McGraw-Hill, 1987.

U.S. Environmental Protection Agency. "Lesson 1: Electrostatic Precipitator Operation." APTI Virtual Classroom SI:412B. 2002. http://yosemite.epa.gov/oaqps/EOGtrain.nsf/fabbfcfe2fc93dac85256afe00483cc4/ca9ae17f9567495885256b66004e7985/$FILE/12bles1.pdf (9/20/05).

Zukeran, Akinori, et al. "Collection Efficiency of Ultrafine Particles by an Electrostatic Precipitator Under DC and Pulse Operating Modes." *IEEE Transactions on Industry Applications* 35, (5): 1184–1190 (1999).

Appendix A
Air Cleaner Selection

The objective of the project described in this report was to conduct experiments and mathematical modeling to determine the effectiveness of room air cleaners in minimizing the impact of an aerosolized biological agent attack on a building. Two types of room air cleaners, a HEPA filter and an electrostatic precipitator (ESP), were tested.

A brief market survey was conducted through the Internet to select representative room air cleaners for this project. It was found that most room air cleaners in the market are certified under the Room Air Cleaner Certification Program, which is sponsored by the Association of Home Appliance Manufacturers (AHAM, ANSI/AHAM AC-1-2002). This standardized measurement procedure was designed to determine the Clean Air Delivery Rate (CADR), indicating how effective a room air cleaner is in reducing concentrations of such particulate pollutants as tobacco smoke, household dust, and pollen.

Approximately 174 different models of room air cleaners from 18 manufacturers are currently certified under the CADR program (AHAM *Directory of Certified Room Air Cleaners*. Edition No. 3, 2004). The specifications of the certified air cleaners were reviewed from the manufacturers' (or venders') Web sites. It was found that among the 174 certified air cleaners, only one was an ESP type air cleaner. Another air cleaner, which has a similar CADR rating as the ESP, was suggested for testing as the filter-type air cleaner. Note that these two air cleaners are also the top two room air cleaners recommended by *Consumer Reports* (2003). The certified CADRs for the two selected air cleaners are summarized in Table A-1.

Table A-1. CADR Values of Selected Air Cleaners

Type	CADR, cfm (m^3/s)		
	Tobacco Smoke (0.09 to 1.0 μm)	Dust (0.5 to 3μm)	Pollen (5 to 11μm)
ESP	300 (.142)	325 (.153)	370 (.175)
HEPA	320 (.151)	330 (.156)	330 (.156)

According to the ANSI/AHAM Standard AC-1, the CADR is the rate of contaminant reduction in a standard test chamber when the test air cleaner is operating, minus the rate of natural decay when the air cleaner is not operating, times the volume of the test chamber. During a certification test, a given quantity of aerosol is generated into the test chamber followed by one minute of mixing with the mixing fan. The test air cleaner is then turned on and the real-time aerosol concentration in the chamber is recorded. The concentration decay inside the chamber is characterized using the following exponential equation:

$$C = C_o e^{-kt} \qquad (1)$$

Where:

C = aerosol concentration at time t, particles/ft^3 (particles/m^3),

C_o = initial aerosol concentration, particles/ft^3 (particles/m^3),

K = overall rate constant of concentration decay, 1/min (1/s), and

t = time, min (s).

The CADR is then calculated as:

$$CADR = V(K - K_n) \qquad (2)$$

Where:

CADR = clean air delivery rate, cfm (m^3/s),

V = volume of test chamber, ft^3 (m^3), and

K_n = the rate constant of the natural concentration decay, without the air cleaner operating, 1/min (1/s).

The following calculations were performed before testing to provide initial estimates based upon available specifications. Since the single-pass efficiency data of the selected air cleaners were not available from the manufacturers, the following analysis was performed to estimate their efficiencies using the reported CADR values. In an initially well-mixed test chamber, the material balance of the test aerosol can be expressed using the following equation:

$$V\frac{dC}{dt} = -C\left(\frac{Q\eta}{100} + uA\right) \qquad (3)$$

Where:

Q = the fan speed of the test air cleaner, cfm (m^3/s),

η = single-pass efficiency, %,

u = the average aerosol terminal-settling velocity, ft/min (m/s), and

A= test chamber area, ft^2 (m^2).

According to Equation (3), concentration decay in the test chamber is controlled by both the intrinsic characteristics of the air cleaner and its test configuration. Integrating Equation (3), one obtains:

$$C = C_o e^{-\frac{\left(\frac{Q\eta}{100} + uA\right)}{V}t} \qquad (4)$$

Where:

$K = (Q\eta/100+uA)/V$ and

$K_n = uA/V$.

Combining Equations (4) and (2), the following equation is obtained:

$$\eta = \frac{CADR}{Q} \times 100 \qquad (5)$$

As shown in Equation (5), the single-pass efficiency can be estimated from both the CADR value and the air cleaner flow rate. It should be noted that this analysis ignores the effect of imperfect mixing induced by the air cleaner. According to the (ANSI/AHAM AC-1-20023) standard, room air cleaners with multi-level fan speeds are tested at the highest setting. The single-pass efficiencies of the ESP for the three different types of aerosols were estimated using Equation (5). The results are summarized in Table A-2. Note that the estimated single-pass efficiency of pollen is slightly over 100%, which is believed to be due to some uncertainties associated with the specified airflow rate.

Table A-2. Estimated Single-Pass Efficiencies for ESP Air Cleaner (Model C-90A)

Aerosol	Single-Pass Efficiency (%)
Tobacco Smoke (0.09 to 1.0 μm)	82
Dust (0.5 to 3μm)	89
Pollen (5 to 11μm)	101

The single-pass efficiencies for the HEPA filter were not estimated because its flow rate specifications were not available from the manufacturer. However, since it is a HEPA filter type, the single-pass efficiency was assumed to be 99%. The maximum flow rate of the air cleaner was then estimated to be 330 cfm (0.156 m^3/s), based on Equation (5).

The specifications of the selected air cleaners, including their flow rates are summarized in Table A-3.

Table A-3. Specifications of Selected Air Cleaners

Type	Fan Flow Rate	Dimensions
ESP	Three levels Low 225 cfm (0.106 m^3/s) Medium 275 cfm (0.130 m^3/s) High 365 cfm (0.172 m^3/s)	0.48m H x 0.38m L x 0.55m W
HEPA	Three levels High 330 cfm[a] (0.156 m^3/s)	0.56m H x 0.46m L x 0.28m W

[a] Estimated by Battelle using Equation (5), by assuming a 99% single-pass efficiency for dust and pollen.

The flow rates of the selected air cleaners were 1.8 to 2.9 times the typical airflow rate of a ventilation system relevant to the Battelle test room, based on the typical 1 cfm/ft^2 (0.0051 $m^3/s/m^2$) standard for an all-air constant-volume ventilation system with ducted returns, and the 128 ft^2 (11.9 m^2) of area for the test facility.

Appendix B
CFD Modeling, Detailed Methodology and Results

B.1. Summary

A computational model was developed and used to evaluate the accuracy and efficacy with which a fluid flow model could successfully predict the concentration evolution of an aerosol injected into a room. The computational fluid dynamics (CFD) package FLUENT was used to implement the model and generate the numerical simulations. The model geometry and flow conditions selected represent one of the test conditions in the test chamber characterization runs performed at Battelle's West Jefferson Facility.

A comparison of numerical predictions to experimental measurements was completed and is documented below in the results section. The agreement is judged sufficiently good to potentially provide guidance on relative trends such as under which conditions select areas in a room will experience higher concentrations than others and the duration of time under which those conditions exist. The results also exhibit good agreement with experiments in terms of the associated decay constant in airborne concentration after the simulant source has been turned off and equipment such as an air cleaner is allowed to continue to remove contaminant from the air. However, in terms of an absolute, highly precise predictor of air concentration, the requisite precision in modeling inputs and the computational expense remain as challenges to using CFD as a general design tool for in-room air contaminant modeling.

B.2. Objective

The ultimate goal of this task is to gain an understanding of how to correctly develop and use computational models to assess the effectiveness of an in-room air cleaner or other HVAC equipment in minimizing the impact of an aerosolized agent attack on a building. There are two principal effects that an indoor air cleaner may have on the evolution of pollutant concentration in a room: enhanced mixing of the room air and cleaning the air by some aerosol removal mechanism. Both of these effects will result in the development of a unique, scenario-, time-, and space-dependent concentration profile in the room of interest. The cost associated with testing all potentially viable HVAC configurations would be prohibitive and logistically complex. Modeling, if properly applied, offers potential savings in identifying the main phenomena that control the effectiveness of in-room air cleaners in reducing the impact of a biological agent dissemination event.

A single simulation was performed under this project, using commercially available software to resolve the effect of air cleaner location on its effectiveness, addressing both the mixing and filtration aspects of the overall effect. This is important because while air filtration acts to reduce pollutant concentration in the room, mixing tends to decrease the pollutant's spatial nonuniformity in the room, thus reducing its concentration at some locations while increasing it at others.

The CFD modeling approach was based on the Eulerian treatment, whereby the contaminant is treated as a continuum fluid dispersing in the air by advection and diffusion processes. The model geometry consisted of a rectangular room with a single air cleaner located near the center of the room, a nebulizer injecting an airborne challenge simulant for a portion of the simulation, one real-time aerosol concentration monitor, and five individual points for monitoring the aggregate mass collected on the filter samples. The indoor air cleaner was treated as a stand-alone interior unit with specified dimensions, flow capacity, and contaminant removal efficiency.

The computer code FLUENT, a well-validated industry standard code for CFD calculations, was applied in this analysis. Using the model geometry and the boundary conditions described in the approach section, a pseudo steady-state three-dimensional solution was obtained for the in-room flow pattern, which was subsequently used to predict a time-dependent contaminant concentration field in the room. A highly resolved spatial and temporal map of the contaminant concentration profile was obtained and compared to experimental data.

B.3. Approach

The steps taken in completing the in-room simulation are as follows:

1. Model Construction – Create a computational mesh that represents all the major features of the experimental configuration.

An illustration of the three-dimensional model geometry is provided in Figure B-1. The complete geometry of the air cleaner, Climet CI-500, the nebulizer, and the room walls were included since their precise features were judged to have the largest impact on subsequent fluid flow patterns. The filter monitoring locations are indicated as open circles, but the physical descriptions themselves were not included in the model.

Dimensions of the room, offset locations of the equipment modeled, and dimensions of the air cleaner intake and exhaust as well as the nebulizer outlet orifice are included in a plan view in Figure B-2a and side or profile view in Figure B-2b. Note that the monitor points representing Filters 1 through 4 were assumed to be 12 inches (0.3 m) from each of the two walls in their respective corners and placed at one of the two elevations indicated, namely 3'6" (1.1 m) or 5'6" (1.7 m) from the floor. The Filter 5 monitoring point was located just above and to one side of the Climet, while the Climet concentration monitor was located 6 inches (0.15 m) above the face center of the top of the unit itself.

2. Boundary Condition Assignments – Specify flow rates for the air cleaner intake and exhaust, the nebulizer mass outflow (including mass fraction of simulant and the time period of operation), and fate indicators on the walls (i.e., whether contaminant that strikes the wall reflects off or is trapped against the surface).

Figure B-1. Model Geometry

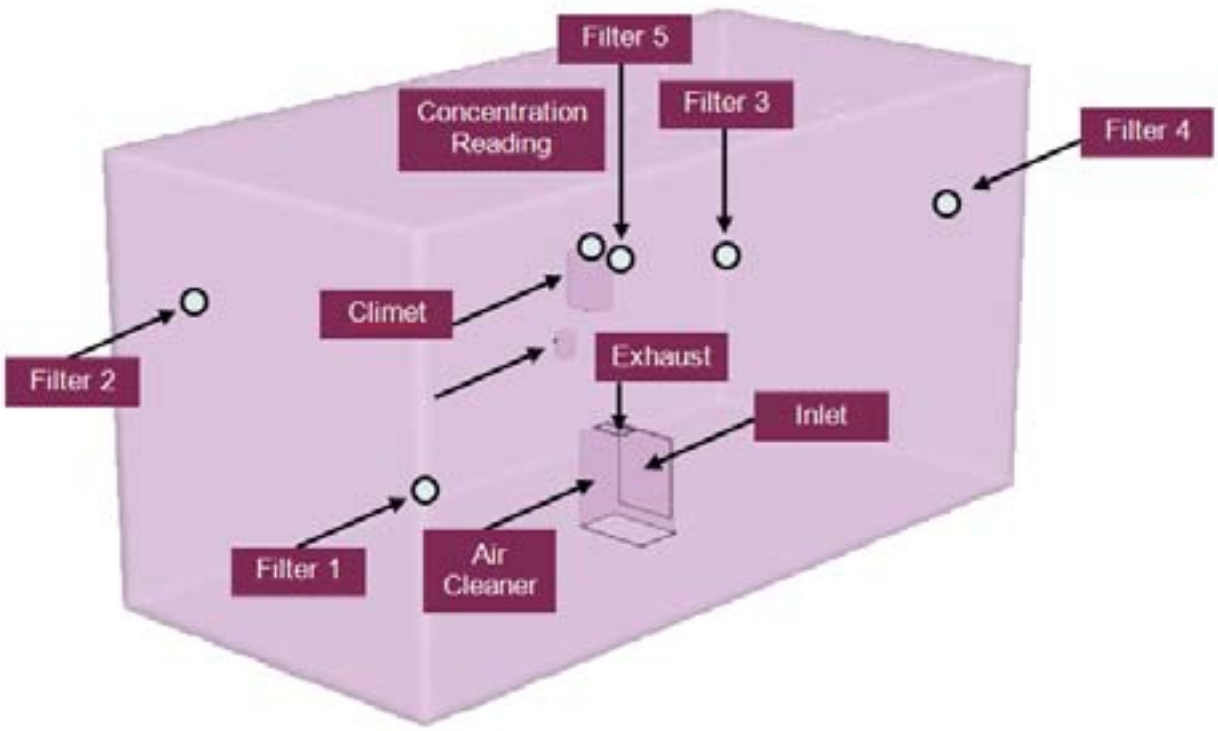

Figure B-2a. Model Dimensions (Plan View)

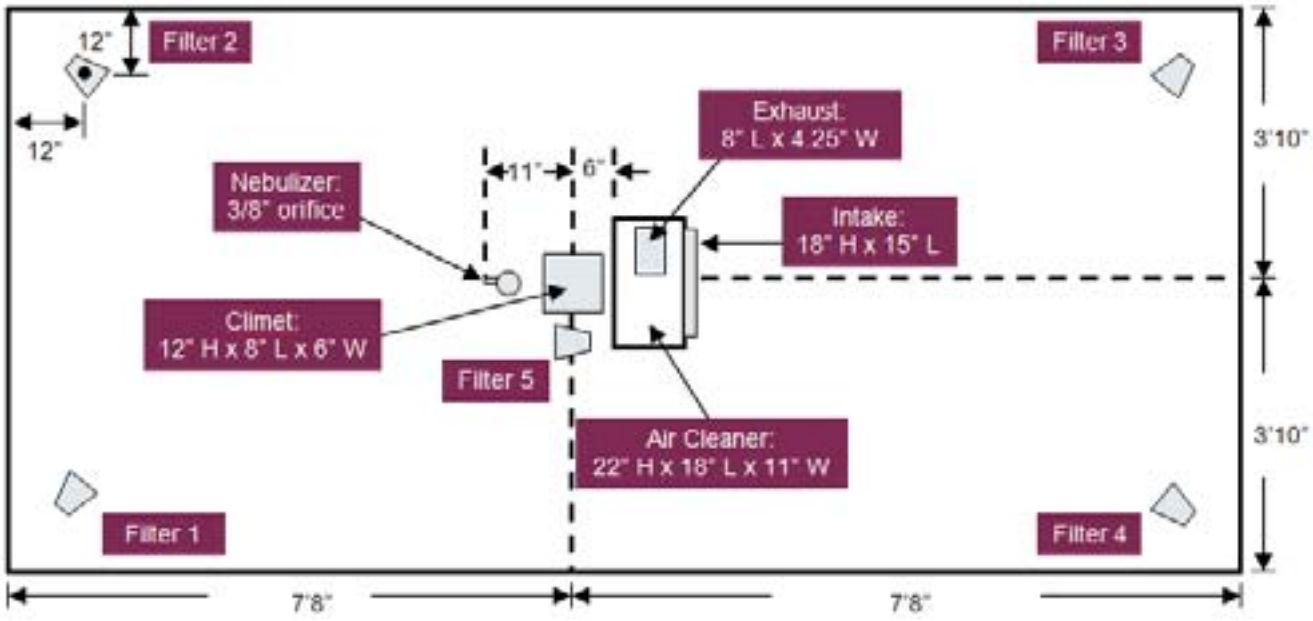

Figure B-2b. Model Dimensions (Side View)

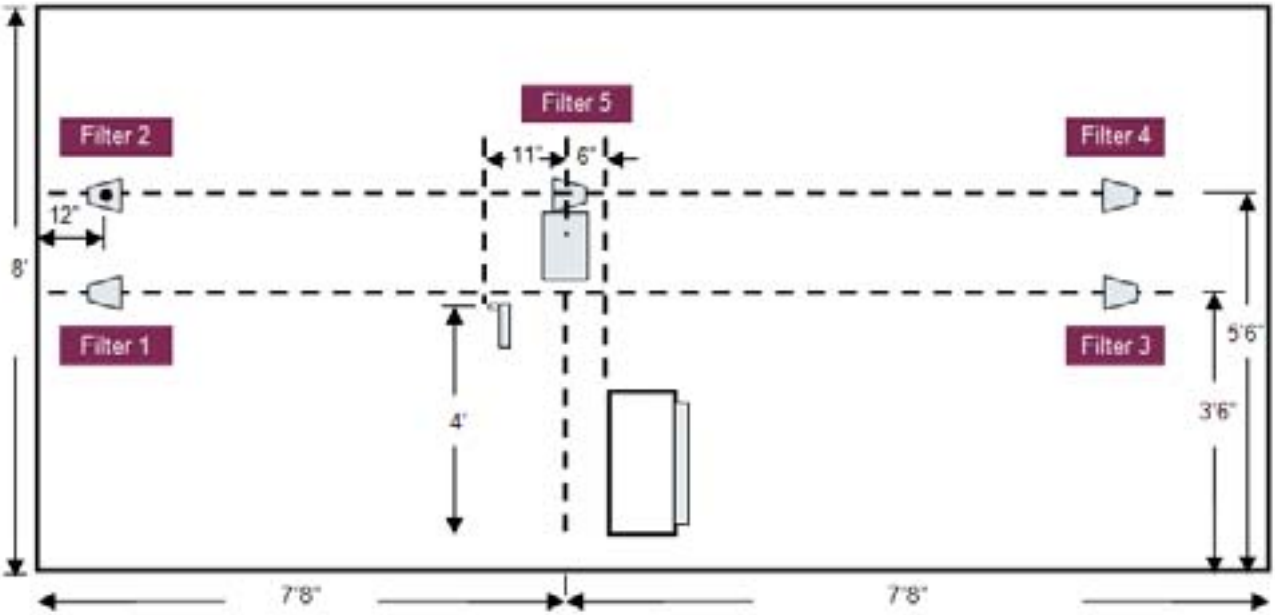

No active HVAC was present, exchanging air inside the room with another compartment or the outside ambience. Therefore, flow rates were assigned to only the air cleaner and the nebulizer, which was assumed to be on for the first 10 minutes of the total 30-minute simulation. The total flow rate assigned to the air cleaner intake was set equal to the sum of the air cleaner exhaust flow rate and the flow rate assigned to the nebulizer (when in operation). The air cleaner was assumed to have perfect efficiency in removing air contaminant, so the intake could be modeled as a domain flow outlet and the exhaust could be represented by an inflow boundary condition.

There are a number of options within FLUENT for specifying the outflow from the air cleaner exhaust and nebulizer orifice as well as the flow rate for the air cleaner intake. The boundary condition specifications that consistently gave the best computational results in terms of mass balance and stability of the solution algorithms are as follows:

- Mass outflow from the air cleaner exhaust corresponding to a flow rate of 450 SCFM (0.212 m^3/s)
- Pressure outlet condition for the air cleaner with a specified target mass flow rate corresponding to 450 SCFM (0.212 m^3/s) with the additional flow attributed to the nebulizer when it is in operation
- Mass outflow from the nebulizer (when in operation) with a specified mass fraction of solids (KCl) content

3. Solver Control Specification – Select for turbulence model, conservation equation closure methods, primitive variable relaxation factors, and solution residual criterion for advancement to the next time step.

A crucial element of the overall success of the model depended upon the choice for turbulence model. Exploratory calculations showed that the flow regime within the room covered all three major regimes, namely laminar, transitional, and fully turbulent. Application of a single turbulence model therefore yielded poor results for both the flow structure as well as the simulant transport. After some trial-and-error application of FLUENT, it was determined that the detached eddy simulation (DES) model gave the physically most realistic results and also preserved numerical stability best for the transient-state calculations. The DES model is a hybrid of the large eddy simulation (LES) and Spallart-Almarus (S-A) models of turbulence. The objective of this type of model is to use LES in the "far field" regions away from flow inlets/outlets and domain boundaries, where the unsteady turbulent motions are directly computed and the smaller scale motions are approximated coupled with S-A near boundaries, a Reynolds-Averaged Navier-Stokes (RANS) one-equation version for kinematic eddy viscosity. Essentially LES is most applicable where the large-scale structure of turbulence is most prevalent while the RANS solver is most applicable to the wall-bounded, small-scale turbulent flow where viscous effects dominate the flow development.

4. Flow Solution – Establish a fully conjugate pseudo steady-state solution followed by a species conservation solution during the injection and cleaning phases of the simulation.

Prior to the transient simulation of the experiment, a steady-state flow solution was obtained to establish the initial conditions under which the test was performed. The steady-state flow field consisted of passage of air through both the air cleaner and nebulizer. When the transient phase of the analysis was conducted, the outlet stream of the nebulizer was replaced with the actual simulant composition. During the process of obtaining the steady-state solution, the base mesh was further refined based on adaptation on velocity magnitude gradient to improve both the fidelity of the solution as well as the convergence properties of the solution. The final mesh consisted of a total of over 1 million cells (see Figures B-3 and B-4).

The steady-state velocity vector flow field is illustrated in Figure B-5. The smaller-scale structure in the flow field is evident from these results. This small-scale structure enhances diffusion mixing in addition to mixing by advection, which in turn promotes more uniform mixing globally. The pathlines of tracer particles released from the nebulizer outlet are given in Figure B-6. Note the persistent tendency for particles to initially travel to Filters 1 and 5. This particle streaming will be reflected in the final results as correspondingly higher aggregate mass recordings as compared to the other filters.

Finally, before initiating the species transport analysis, a separate analysis was conducted to estimate the diffusion coefficient. Turbulent diffusion will dominate in the fully turbulent portion of the flow and advection will dominate in the laminar flow regions; nonetheless, molecular diffusion will play an important role in transport for the transitional flow regime. The transitional flow (roughly on the order of 0.1 to 0.25 m/s in velocity magnitude for this problem) comprises a significant portion of the entire flow spectrum, as can be seen in Figure B-5, and should not be neglected. The value calculated for the diffusion coefficient from the Chapman-Enskog equation agreed very well with the diffusion coefficient generated from the kinetic model in FLUENT. For simplicity, water was chosen as the surrogate for the solids species in the simulation injection stream because its diffusion parameters are much better characterized. Since water was the solvent for the KCl simulant, and the correct mass fraction was used, little error is expected to be incurred due to this simplification.

5. Monitor time-dependent concentration predictions for the Climet and filters as well as a time-integrated collected mass estimates for the filters.

The simulant concentration was recorded at the end of each time step for the locations in the model domain corresponding the Climet sample and Filters 1 through 5. The concentration data were then integrated with respect to time to get the cumulative collected mass on each of the filters.

Figure B-3. Model Mesh with Outlines of Face Cells Illustrated

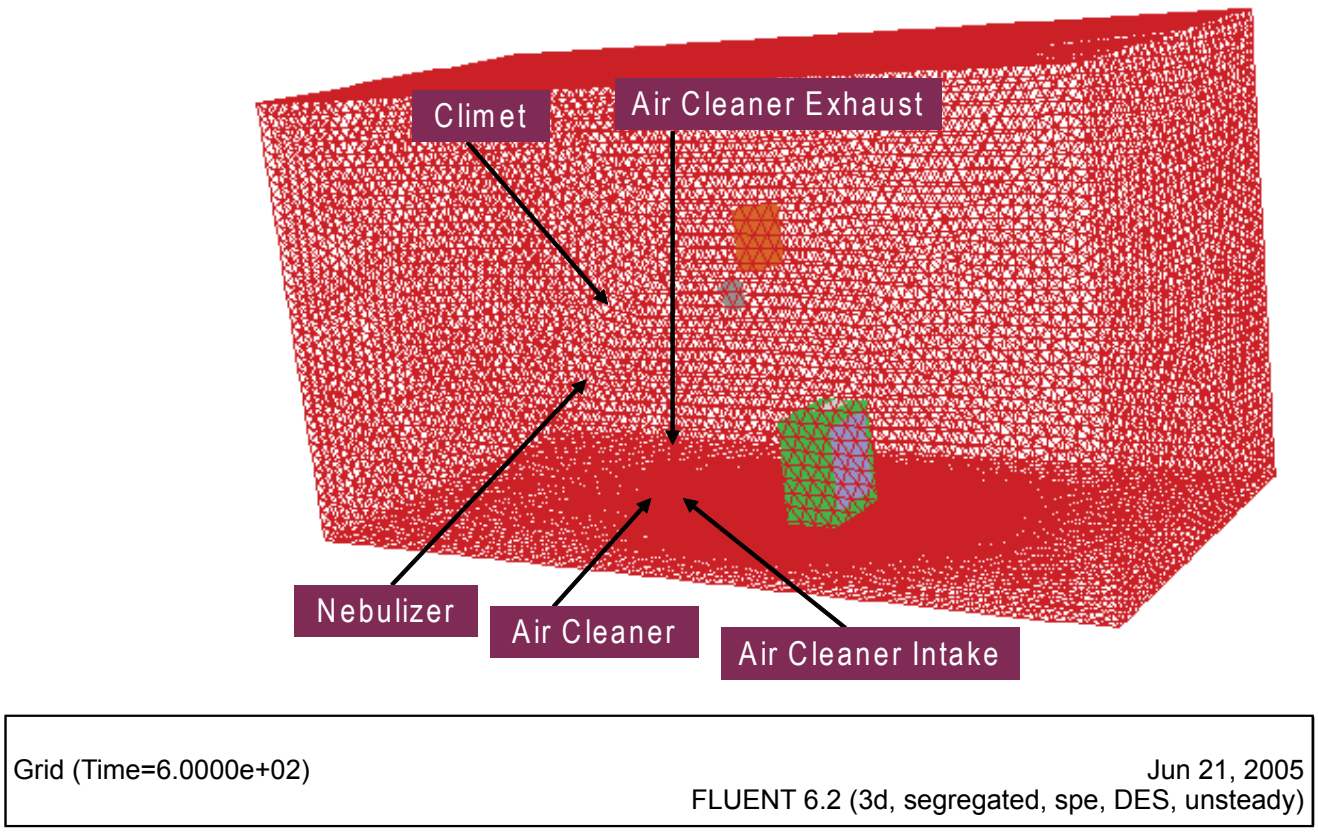

Figure B-4. Cells From the Base Mesh Marked for Adaptive Refinement

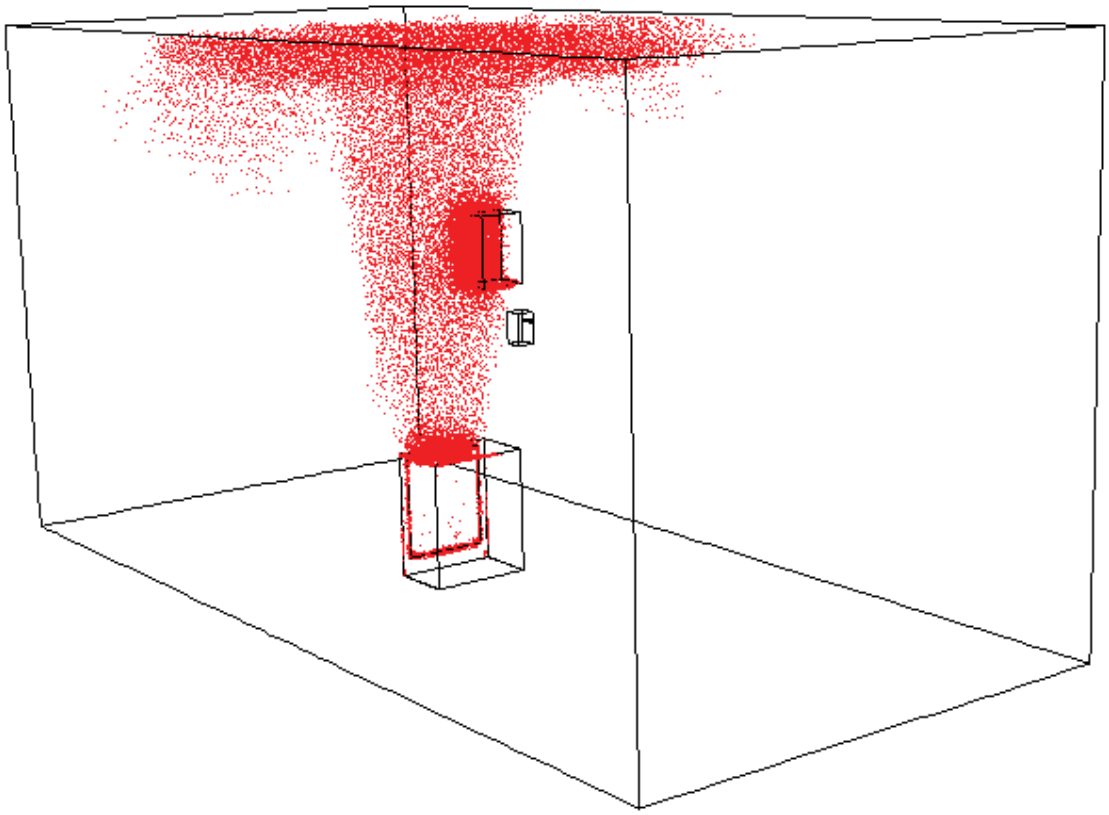

Figure B-5. Velocity Vector Flow Field

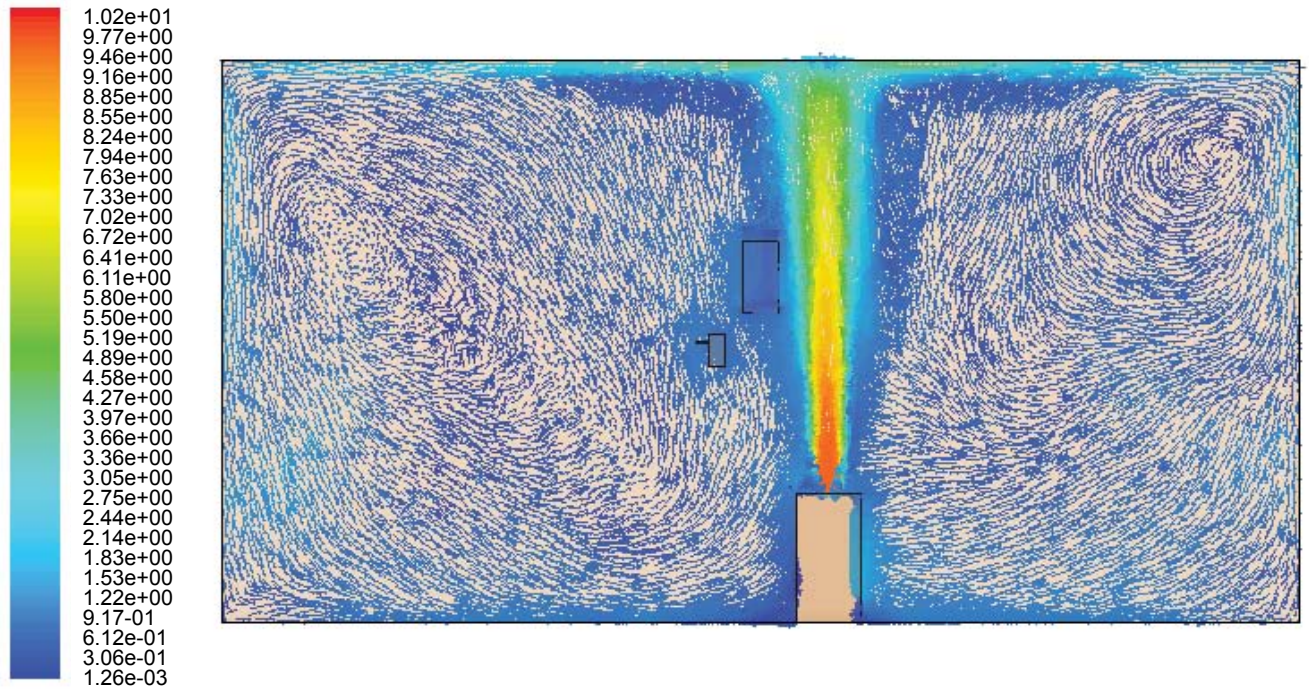

Velocity Vectors Colored By Velocity Magnitude (m/s) (Time=7.3011e+01) Jul 25, 2005
FLUENT 6.2 (3d, segregated, DES, unsteady)

Figure B-6. Updated Pathlines (Colored by Total Residence Time)

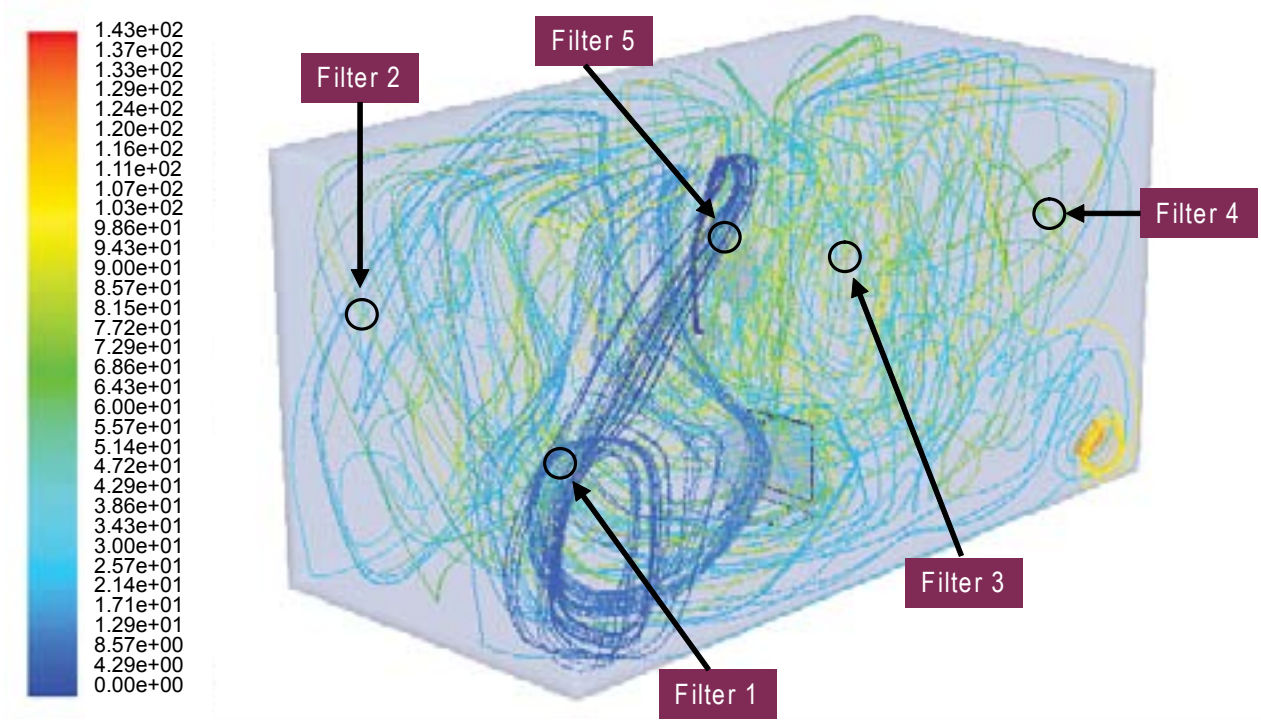

Path Lines Colored by time (s) (Time=7.5101e+01) Jul 25, 2005
FLUENT 6.2 (3d, segregated, spe, DES, unsteady)

B.4. Results

In order to accelerate the computations, the flow field established in the steady-state solution was held constant and the solution proceeded by iterating on the species balance equations for the water and solids content of the injected simulant. The simulation began with a 600-second phase during which the nebulizer was continuously injecting simulant into the room air space at a constant flow rate, followed by a 20-minute period during which the nebulizer was turned off and the air cleaner operated at 450 SCFM (0.212 m^3/s), assuming 100% removal efficiency.

The results of the species concentration predictions are graphically presented in Figure B-7 (half-plane passing through the nebulizer) and Figure B-8 (planes passing through the two filter elevations) at the very end of the 600-second period just prior to turning off the nebulizer.

The concentration field 20 minutes later with the nebulizer turned off and the air cleaner continuously running is provided in Figures B-9 and B-10 (nebulizer half-plane and filter elevation planes, respectively). Note that in the time interval following shut-down of the nebulizer and continued operation of the air cleaner, the concentration field of simulant becomes more homogeneous.

The predicted concentration of simulant as a function of time for the Climet and the five filter locations are given in Figure B-11. From the data presented in Figure B-11, the decay constants predicted from the model were computed and compared to experimentally observed values as well as to the value derived from an analytical model assuming perfect mixing within the room. Table B-1 provides a comparison of the experimental, model, and well-mixed approximation results.

Figure B-7. KCl Concentration With Nebulizer at 10 Minutes of Operation

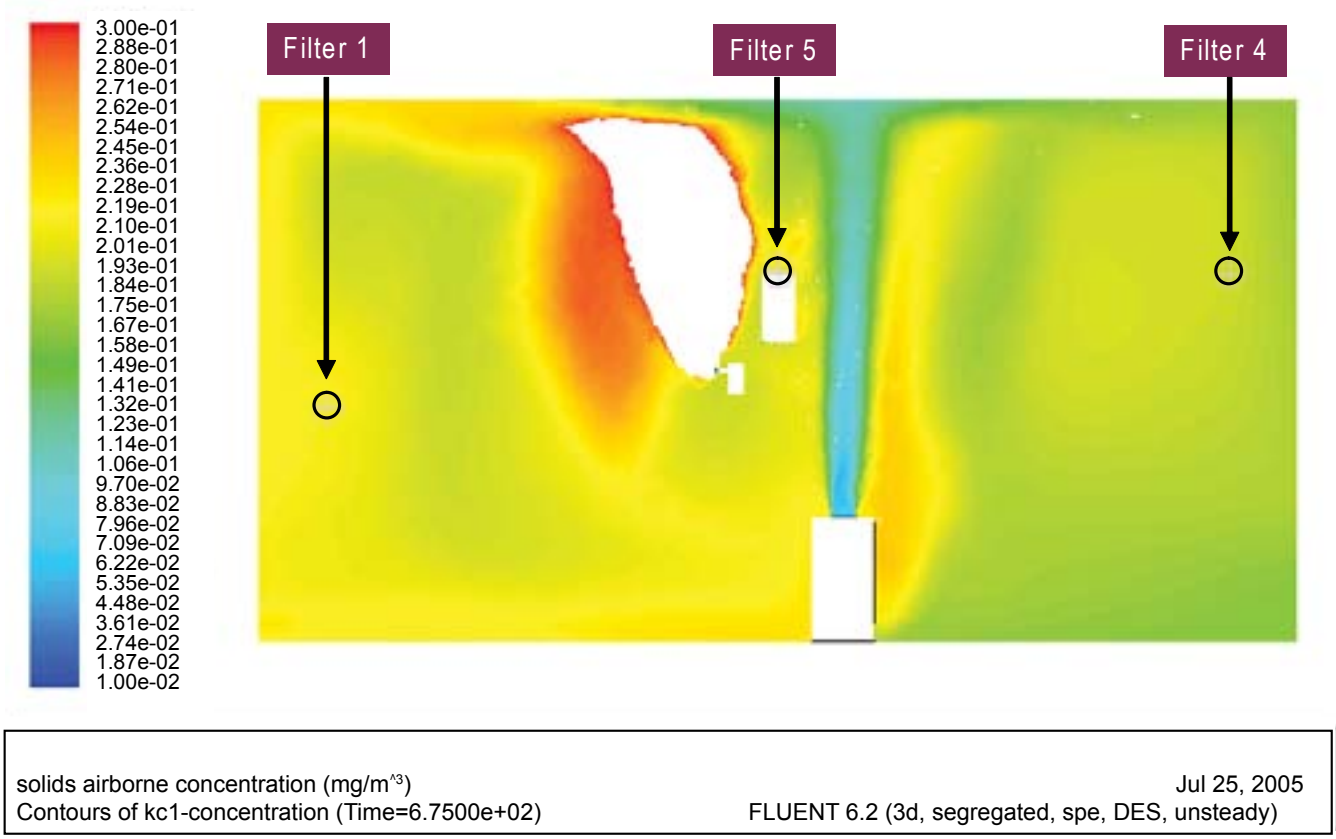

Figure B-8. KCl Concentration With Nebulizer at 10 Minutes of Operation (Cont'd)

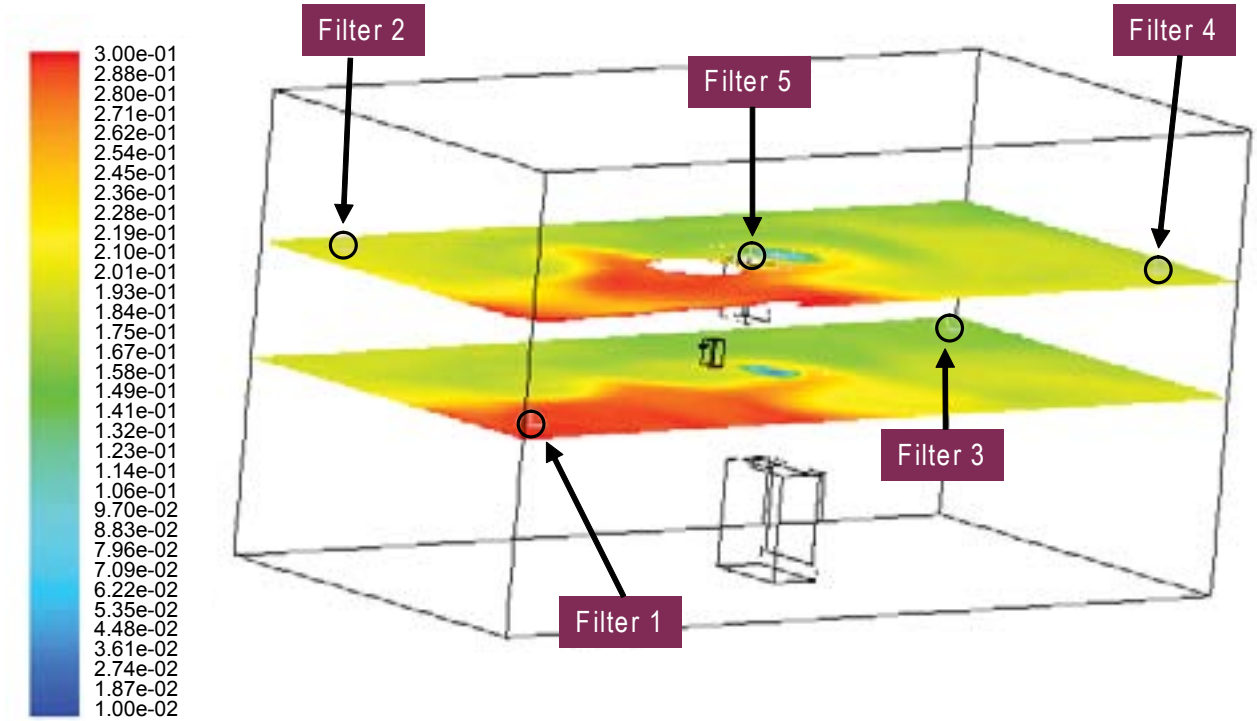

solids airborne concentration (mg/m^3) Jul 25, 2005
Contours of kc1-concentration (Time=6.7500e+02) FLUENT 6.2 (3d, segregated, spe, DES, unsteady)

Figure B-9. KCl Concentration after 20 Minutes of Air Cleaner Operation (No Nebulizer)

solids airborne concentration (mg/m^3) Jul 25, 2005
Contours of kc1-concentration (Time=1.3140e+03) FLUENT 6.2 (3d, segregated, spe, DES, unsteady)

Figure B-10. KCl Concentration after 20 Minutes of Air Cleaner Operation (No Nebulizer)

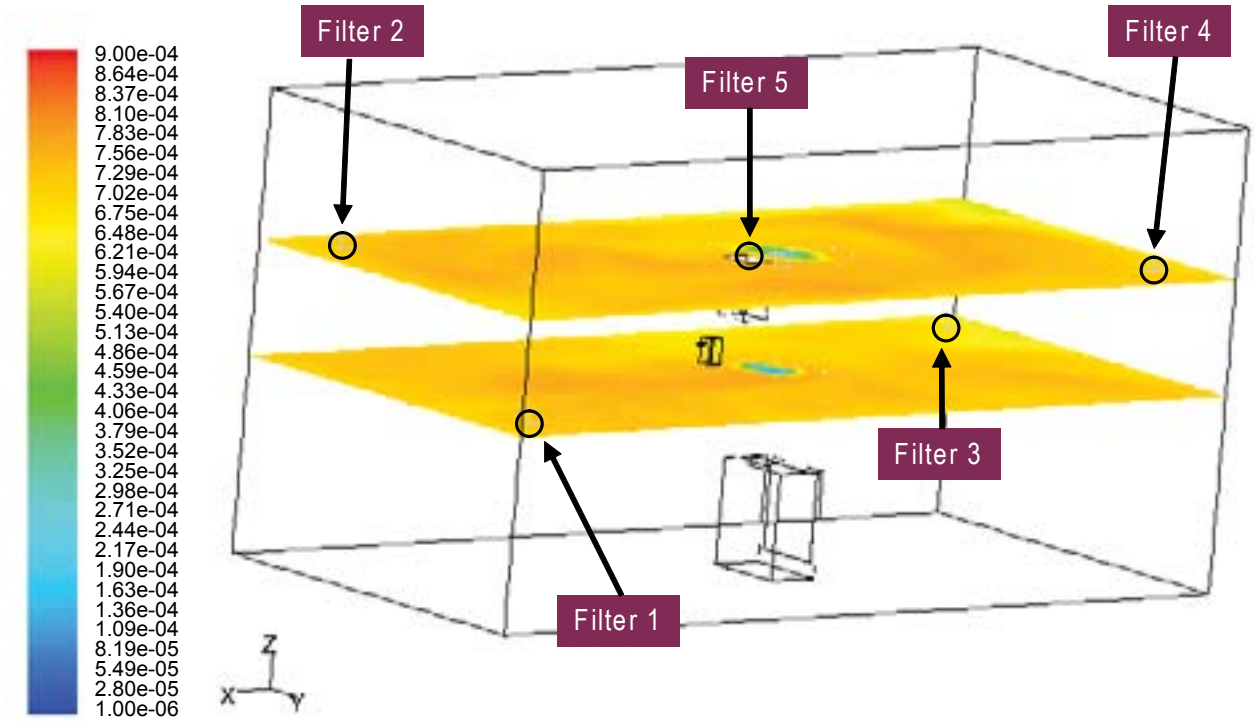

solids airborne concentration (mg/m^3) Jul 25, 2005
Contours of kc1-concentration (Time=1.3140e+03) FLUENT 6.2 (3d, segregated, spe, DES, unsteady)

The collected mass predicted for each filter was computed and compared to the collected data samples from the experiment in Figure B-12. Note that there are two sets of data compared to the experimental results: the unaltered results from the CFD predictions and the results from CFD renormalized to yield the same average collected mass as reported in the experiment (6×10^{-4} g). The normalization process is somewhat justified by the fact that (1) there are some uncertainties in the stated flow rate of solids from the nebulizer, (2) the species equation was completely decoupled, and (3) without a comprehensive turbulence model for the class of flow problem, a trends analysis is the most valuable contribution from this type of simulation. A numerical comparison of the experimental to normalized collected mass values is given in Table B-2. The only large deviation is recorded for Filter 5, located near the Climet.

Table B-1. Comparison of Decay Constants for Experiment versus Model Predictions.

	Experiment	Model	Well-Mixed Assumption
Average Decay Constant, *k* (1/min)	0.289	0.535	0.501

Table B-2. Comparison of Experimental to Predicted Values for Collected Mass Values.

	Experimental (g)	Model (g)	Model Normalized (g)	% Deviation Experimental vs. Normalized (%)
Filter 1	8.20E-04	1.20E-03	7.98E-04	3
Filter 2	7.00E-04	8.10E-04	5.39E-04	23
Filter 3	5.50E-04	6.87E-04	4.57E-04	17
Filter 4	5.25E-04	7.92E-04	5.27E-04	0
Filter 5	4.10E-04	1.03E-03	6.84E-04	-67
Average	6.01E-04	9.03E-04	6.01E-04	0

Figure B-11. KCl Concentration versus Time

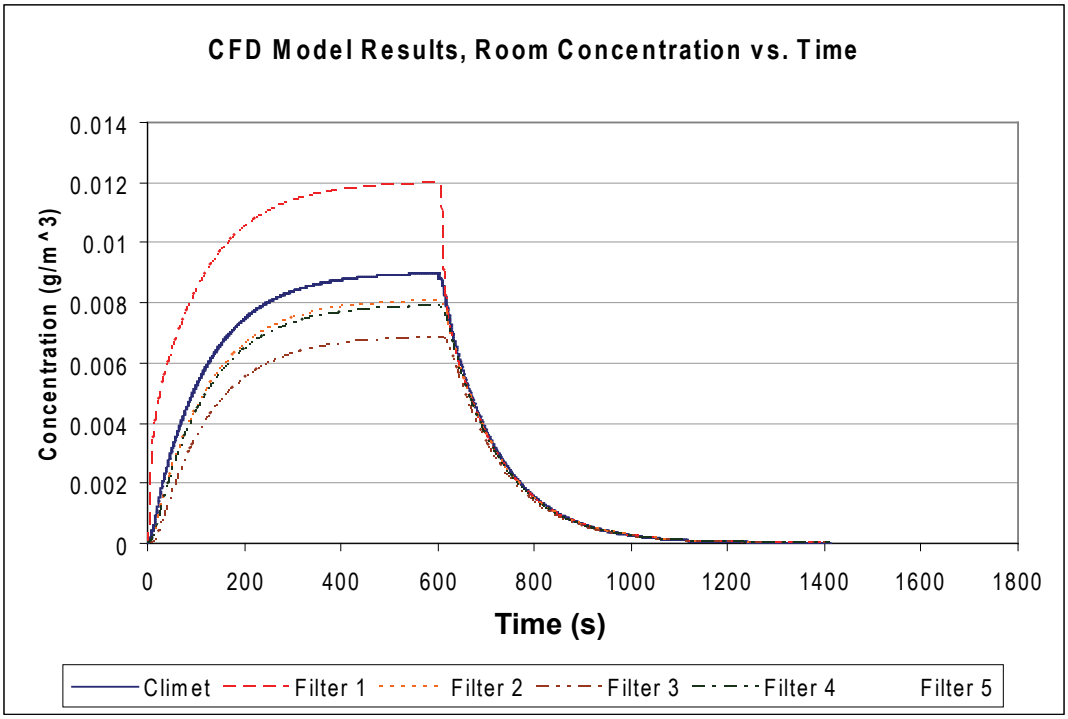

Figure B-12. Collected Mass of KCl in Filters

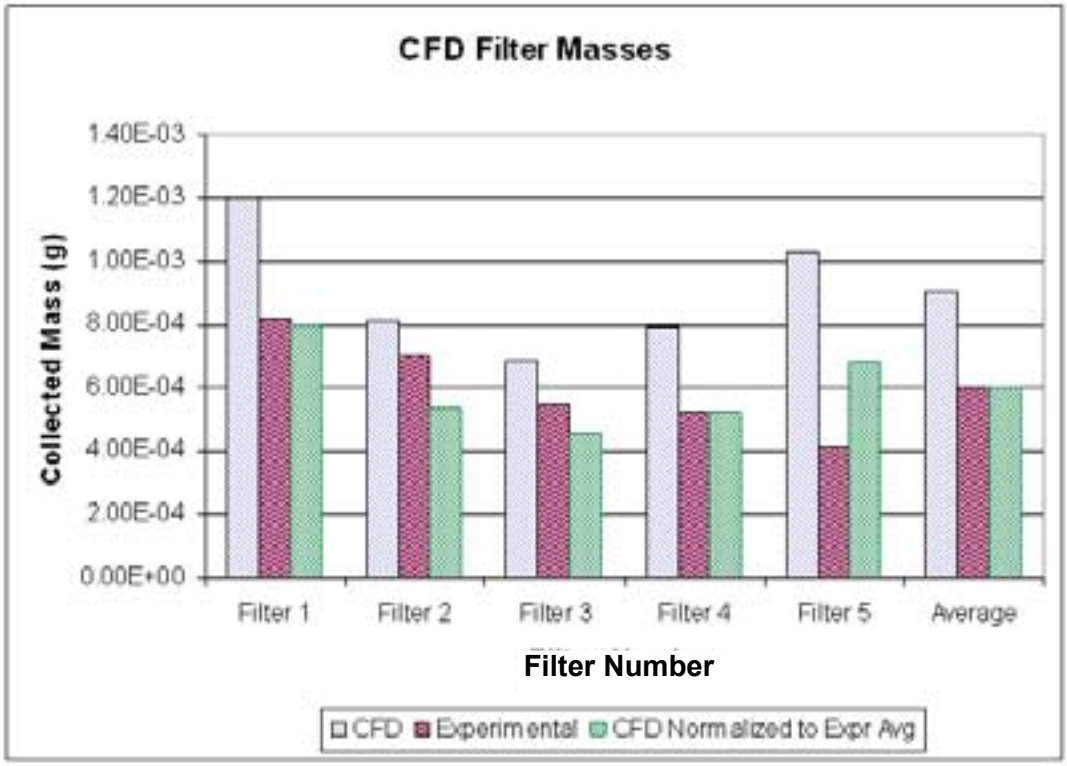

B.5. Conclusions and Recommendations

CFD simulation has been demonstrated here as a potentially viable means of obtaining spatially and temporally highly resolved estimates of the concentration field for an in-room release scenario. The normalized predictions agreed well with experimentally measured results ranging from 3% to 23% difference with the exception of one filter sample, which recorded a 67% difference. The predictions also generally demonstrated the correct trends in terms of which filters recorded the greatest amount of accumulated mass (again with the exception of one outlier filter).

The model exhibited a large difference in the average decay constant as compared to the experimentally determined value while comparing very favorably to the value obtained from the well-mixed approximation. There could be a number of reasons why the removal rate is more compatible with the well-mixed theory than the experimental results:

- Source rate of KCl Simulant. There is the potential for vaporization of water inside the nebulizer, resulting in a lower actual emission rate of aerosolized KCl in solution as compared to the assumed value in the model. Recognition of this fact was one of the primary motivations for renormalizing the model results to reflect the average collected mass from the experiments. However, renormalization will have relatively little impact on the calculated value for the decay constant. Uncertainty in the solids source rate would have a significant influence on decay constant if the rate varied appreciably with time.
- Air Cleaner Flow Rate. The rated flow rate of the air cleaner is 330 CFM, whereas the model assumed a rate of 450 cfm (0.212 m^3/s). Periodic measurement, however, consistently indicated a flow rate in the range of 425 to 450 cfm (0.201 to 0.212 m^3/s) in the experiments. Nonetheless, if the flow rate varied with time, or the actual cleaner collection efficiency (assumed to be 100% in the model) was significantly less at the high flow rate as compared to the rated flow rate of the device, then significant variations between predicted and measured concentration as a function of time could be observed.
- Limitations in the Turbulence Model. Only the large-scale turbulence is explicitly calculated, whereas the small-scale structure is modeled using an empirical one-equation expression for closure. If the small-scale turbulence is over-estimated with this high-Reynolds number model, then predictions will reflect a higher degree of mixing than actually takes place.
- Decoupling the Species and Flow Field Solutions. It is not immediately obvious what the magnitude of the effect is by first solving the flow field and then the species balance equations separately. Presumably the largest impact would be the decoupling of the species balance and the equation of turbulent viscosity. However, this should result in a global change in concentration level and therefore is expected to have little impact on the average decay constant.

Due to the large computational expense incurred by this type of modeling effort, CFD simulation of in-room contaminant transport when the flow is transitional (neither laminar nor fully turbulent) should be used judiciously. Currently, the explicit computation and resolution of large-scale turbulence can only be done time-dependent. Until such time as there are good flow-averaging methods such as RANS for the Navier-Stokes equations with closure expressions (otherwise known as models) for turbulence that can accurately capture large-scale turbulence in the transition region, problems of this class will be computationally expensive to simulate.

Nonetheless, CFD offers a high degree of modeling flexibility and as many monitor locations as desired can be specified with negligible additional computational expense. As the turbulence modeling capabilities improve, CFD will offer the potential for generating spatially resolved simulations of contaminant transport that cannot be replicated by lumped-parameter or zonal models that assume homogeneously mixed compartments. Therefore, application of CFD can be a viable alternative to conducting experiments with either complex and expensive HVAC requirements or a large number of measurements with high record frequencies.

Appendix C
Quality Assurance

Work under this project was completed in accordance with the EPA-approved quality assurance test plan (QAPP) entitled "Research on Air Cleaning and HVAC Systems for Protecting Buildings From Terrorist Attacks; Test/Quality Assurance Plan for Task 4: Evaluation of In-Room Air Cleaners." The QAPP describes the test procedures, and data handling and analysis procedures. These procedures are also described throughout this report. The QAPP also describes the quality objectives and quality assurance (QA) procedures, some of which are listed below:

- Before performing the single-pass efficiency tests, the concentration was confirmed to be uniform with a coefficient of variation (CV) of 15% or less across the air cleaner inlet.
- Duplicate tests were performed with individual measurements not deviating from the average by more than 15%.
- Filters were allowed to equilibrate in a humidity-controlled room for 24 hours before weighing, blank (untested) filters were carried with all sample filters, and all filters were weighed at least three times.

As an example, the data from the concentration uniformity measurement is shown in Table C-1. The total particle concentration was measured with the scanning mobility particle sizer (SMPS) three times each at nine different locations. The sampling location was varied over the course of the one-hour test period in order to determine both temporal and spatial variability in concentration. As shown in Table C-1, the temporal variability in concentration was low, with a CV of less than 3% at all sampling locations. The spatial variability was a bit higher, however, with an average concentration of 19,700 particles per cm^3 and a standard deviation of 2,600 particles per cm^3 leading to a CV of 13.2%. Additional QA calculations can be found throughout the body of the report.

Table C-1. Concentration Uniformity: Average of Three Measurements at Each Location

Average Concentration (particles/cm^3) Coefficient of Variation		
1.93E+04 CV - 2.1%	1.75E+04 CV - 1.0%	1.56E+04 CV - 1.0%
2.21E+04 CV - 2.8%	1.88E+04 CV - 0.8%	1.78E+04 CV - 0.9%
2.39E+04 CV - 2.8%	2.16E+04 CV - 2.9%	2.05E+04 CV - 0.5%

As outlined in the QAPP, an internal QA audit of laboratory procedures and data was performed by a Battelle QA officer. The results of this audit were communicated to the Battelle quality assurance manager and project manager as well as the EPA project manager. No significant corrective actions were required from this audit. At the completion of this project, all quality objectives had been achieved.

EPA/600/R-08/12 | January 2008 | www.epa.gov/ord

United States
Environmental Protection
Agency

Office of Research and Development
National Homeland Security Research Center
Cincinnati, OH 45268

PRESORTED STANDARD
POSTAGE & FEES PAID
EPA
PERMIT NO. G-35

Official Business
Penalty for Private Use
$300

Recycled/Recyclable
Printed with vegetable-based ink on
paper that contains a minimum of
50% post-consumer fiber content
processed chlorine free